


January 2012

Metal Oxide Graphene Nanocomposites for Organic and Heavy Metal Remediation

Tanvir E. Alam

University of South Florida, tanvir@mail.usf.edu

Follow this and additional works at: <http://scholarcommons.usf.edu/etd>

 Part of the [American Studies Commons](#), [Materials Science and Engineering Commons](#), [Mechanical Engineering Commons](#), and the [Nanoscience and Nanotechnology Commons](#)

Scholar Commons Citation

Alam, Tanvir E., "Metal Oxide Graphene Nanocomposites for Organic and Heavy Metal Remediation" (2012). *Graduate Theses and Dissertations*.

<http://scholarcommons.usf.edu/etd/3945>

This Thesis is brought to you for free and open access by the Graduate School at Scholar Commons. It has been accepted for inclusion in Graduate Theses and Dissertations by an authorized administrator of Scholar Commons. For more information, please contact scholarcommons@usf.edu.

Metal Oxide Graphene Nanocomposites for Organic and Heavy Metal Remediation
Application

by

Tanvir E Alam

A thesis submitted in partial fulfillment
of the requirements for the degree of
Master of Science in Mechanical Engineering
Department of Mechanical Engineering
College of Engineering
University of South Florida

Co-Major Professor: Ajit Mujumdar, Ph.D.
Co-Major Professor: Manoj K. Ram, Ph.D.
Ashok Kumar, Ph.D.

Date of Approval:
March 6, 2012

Keywords: Nanomaterial, Adsorption, Photocatalytic activity, Nanosorbents,
Nanocatalysts

Copyright © 2012, Tanvir E Alam

Dedication

I dedicate this work to my beloved parents, family and my friends.

Acknowledgement

I am thankful to everyone who helped me throughout my research work to make this work successful. I thank my family for their love and constant support. I express my heartiest gratitude and thankfulness to Dr. Ajit Mujumdar, Major Professor and to Dr. Manoj K Ram, Co-major Professor for providing me with this opportunity to conduct the thesis and also for their guidance and encouragement throughout my research work. I am grateful to Dr. Ashok Kumar for accepting to be in the committee and also give me the valuable guidance when required. I am very thankful to my colleagues and friends in the group; especially, Mikhail Ladanov, Pedro J. Villalba, and Yang Yang Zhang for their valuable suggestions and help during the research work and Atiquzzaman for his support and encouragement. Also, I would like to thank Department of Mechanical Engineering for the financial support.

Table of Contents

| | |
|--|------|
| List of Tables | iii |
| List of Figures | iv |
| Abstract | viii |
| Chapter1 Introduction | 1 |
| 1.1 Overview of Nanocomposite Materials | 1 |
| 1.1.1 Overview of Graphene | 2 |
| 1.1.2 Overview of Metal Oxides | 4 |
| 1.1.2.1 Titanium Dioxide | 4 |
| 1.1.2.2 Silicon Dioxide | 5 |
| 1.2 Applications of Nanocomposite Materials | 5 |
| 1.3 Water Decontamination Process | 7 |
| 1.4 Photocatalysis | 10 |
| 1.5 Adsorption | 11 |
| 1.6 Research Aims | 11 |
| 1.6.1 Overall Objective of the Study | 11 |
| 1.7 References | 12 |
| Chapter 2 Characterization Tools | 16 |
| 2.1 Raman Spectroscopy | 16 |
| 2.2 Scanning Electron Microscopy | 17 |
| 2.3 Energy Dispersive Spectroscopy | 19 |
| 2.4 X-Ray Diffraction (XRD) | 19 |
| 2.5 Transmission Electron Microscope (TEM) | 21 |
| 2.6 Fourier Transform Infrared Spectroscopy (FTIR) | 22 |
| 2.7 UV-Visible Spectroscopy | 23 |
| 2.8 References | 24 |
| Chapter 3 Synthesis, Characterization of G-TiO ₂ and Application in Organic Material Remediation | 26 |
| 3.1 Introduction | 26 |
| 3.2 Materials for G-TiO ₂ | 27 |
| 3.3 Synthesis of G-TiO ₂ Nanocomposite | 27 |
| 3.4 Flow Diagram of the Process | 28 |
| 3.5 Characterization of G-TiO ₂ | 29 |
| 3.5.1 Machine Specification and Sample Preparation | 29 |

| | |
|--|----|
| 3.5.2 Raman Spectroscopy | 29 |
| 3.5.3 Transmission Electron Microscopy | 30 |
| 3.5.4 Fourier Transform Infrared (FTIR) Spectroscopy | 35 |
| 3.5.5 UV-Visible Spectroscopy | 36 |
| 3.5.6 X-Ray Diffraction | 37 |
| 3.6 Organic Material Remediation Using G-TiO ₂ Nanocomposite | 38 |
| 3.6.1 Photocatalytic Measurement | 39 |
| 3.6.2 Finding of the Work | 41 |
| 3.7 Summary | 48 |
| 3.8 References | 49 |
| | |
| Chapter 4 Synthesis, Characterization of G-SiO ₂ and Application in Heavy Metal Removal | 52 |
| 4.1 Introduction | 52 |
| 4.2 Materials for G-SiO ₂ | 53 |
| 4.3 Synthesis of G-SiO ₂ Nanocomposite | 54 |
| 4.4 Flow Diagram of the Process | 54 |
| 4.5 Characterization of G-SiO ₂ | 55 |
| 4.5.1 Machine Specification and Sample Preparation | 55 |
| 4.5.2 Raman Spectroscopy | 56 |
| 4.5.3 Fourier Transform Infrared (FTIR) Spectroscopy | 57 |
| 4.5.4 Scanning Electron Microscope (SEM) | 58 |
| 4.5.5 Transmission Electron Microscopy | 61 |
| 4.5.6 X-Ray Diffraction | 64 |
| 4.5.7 Cyclic Voltammetry | 65 |
| 4.5.8 I-V Characteristic | 65 |
| 4.6 Heavy Metal Remediation from Water Using G-SiO ₂ | 70 |
| 4.6.1 Adsorbate Solution and Adsorbent Preparation | 70 |
| 4.6.2 Experimental Setup | 72 |
| 4.6.3 Finding of the Work | 72 |
| 4.7 Summary | 79 |
| 4.8 References | 79 |
| | |
| Chapter 5 Conclusion and Future Recommendation | 82 |
| 5.1 Organic Material Remediation | 83 |
| 5.2 Heavy Metal Removal | 83 |
| 5.3 Future Recommendation | 85 |
| | |
| Appendix A: Permissions | 86 |

List of Tables

| | |
|---|----|
| Table 1.1: Comparison between different allotropes of carbon | 4 |
| Table 1.2: Review of conventional technologies employed for water purification | 8 |
| Table 1.3: Advantage and disadvantages of different heavy metal removal techniques | 9 |
| Table 3.1: Concentration change with irradiation time under UV-visible (30 W/ m ²). | 42 |
| Table 3.2: Concentration change with irradiation time under normal soft Light | 45 |
| Table 4.1: The parameters for the G-SiO ₂ synthesis | 54 |
| Table 4.2: Change of the redox peak value with respect to time for 0.07 M ZnCl ₂ | 73 |
| Table 4.3: Change of the redox peak value with respect to time for 0.02 M ZnCl ₂ | 78 |

List of Figures

| | |
|--|----|
| Figure 1.1: Mother of all graphitic forms. | 3 |
| Figure 1.2: Mechanism of the photocatalytic effect of TiO ₂ | 10 |
| Figure 2.1: Renishaw Raman Spectrometer at USF | 17 |
| Figure 2.2: Shows the basic block diagram of a Scanning Electron Microscope. | 18 |
| Figure 2.3: Scanning Electron Microscopy (SEM) and Energy Dispersive Spectroscopy (EDS) at USF | 19 |
| Figure 2.4: X-Ray Diffraction machine at USF | 20 |
| Figure 2.5: Transmission Electron Microscope at USF | 21 |
| Figure 2.6: Fourier Transform Infrared Spectroscopy at USF | 23 |
| Figure 2.7: UV Visible Spectroscopy at USF | 24 |
| Figure 3.1: Flow diagram of G-TiO ₂ synthesis process | 28 |
| Figure 3.2: Raman spectra of G-TiO ₂ nanocomposite | 30 |
| Figure 3.3: TEM image of G-TiO ₂ (20 nm) | 31 |
| Figure 3.4: TEM image of G-TiO ₂ (50 nm) | 32 |
| Figure 3.5: HRTEM image of G-TiO ₂ (10 nm) | 33 |
| Figure 3.6: HRTEM image of G-TiO ₂ (5 nm) | 34 |
| Figure 3.7: FTIR spectra of G-TiO ₂ nanocomposites | 35 |
| Figure 3.8: UV-visible absorption spectra of TiO ₂ (p25),G-TiO ₂ nanocomposites. | 36 |
| Figure 3.9: X-Ray diffraction pattern of G-TiO ₂ | 37 |

| | |
|---|----|
| Figure 3.10: Mechanism of the photocatalytic effect of G-TiO ₂ | 39 |
| Figure 3.11: G-TiO ₂ coated petri dish | 40 |
| Figure 3.12: G-SiO ₂ coated petri dish | 40 |
| Figure 3.13: TiO ₂ coated petri dish | 41 |
| Figure 3.14: Photodegradation of MO by G-TiO ₂ , G-SiO ₂ and commercially available P25 under irradiation of 30 W/m ² UV-visible light | 43 |
| Figure 3.15: Samples collected after certain irradiation time intervals for G-TiO ₂ | 44 |
| Figure 3.16: Samples collected after certain irradiation time intervals for P25 | 44 |
| Figure 3.17: Samples collected after certain irradiation time intervals for P25 | 44 |
| Figure 3.18: Coated petri dish with G-TiO ₂ (a) and P25 (b) for photodegradation of MO under irradiation of 60 W normal | 46 |
| Figure 3.19: Setup for photodegradation of MO by G-TiO ₂ under irradiation of 60 W normal bulb | 46 |
| Figure 3.20: Setup for photodegradation of MO by P25 under irradiation of 60 W normal bulb | 47 |
| Figure 3.21: Photodegradation of MO by G-TiO ₂ and commercially available P25 under irradiation of 60 W normal bulb | 48 |
| Figure 4.1: Flow diagram of G-SiO ₂ synthesis process | 54 |
| Figure 4.2: Raman spectra of G-SiO ₂ for samples (S1, S2, S3 indicates different ratio of graphene and G-SiO ₂). | 56 |
| Figure 4.3: FTIR spectra of S1, S2, S3 (G-SiO ₂ nanoparticles) and SiO ₂ nanoparticles | 57 |
| Figure 4.4: SEM image of G-SiO ₂ (which indicates S1 composition) | 58 |
| Figure 4.5: SEM image of G-SiO ₂ (which indicates S2 composition) | 59 |
| Figure 4.6: SEM image of G-SiO ₂ (which indicates S3 composition) | 60 |
| Figure 4.7: TEM image of G-SiO ₂ (10% graphene -90% SiO ₂) at 100 nm scale | 61 |

| | |
|--|----|
| Figure 4.8: TEM image of G-SiO ₂ (10% graphene -90% SiO ₂) at 20 nm scale | 62 |
| Figure 4.9: High resolution TEM image of G-SiO ₂ (10% graphene – 90% SiO ₂) | 63 |
| Figure 4.10: XRD of different amount of G-SiO ₂ | 64 |
| Figure 4.11: Cyclic voltammetry of G-SiO ₂ (S1, S2 and S3) coated on ITO glass plate as working electrode, platinum as counter and Ag/AgCl as reference electrode in 0.1M TEATFF ₄ ⁻ in acetonitrile solution | 65 |
| Figure 4.12: Current –Voltage characteristics of G-SiO ₂ samples (S1, S2, S3) at room temperature | 66 |
| Figure 4.13: Current –Voltage characteristics of G-SiO ₂ samples S1 at different temperature. | 67 |
| Figure 4.14: Current –Voltage characteristics of G-SiO ₂ samples S2 at different temperature | 68 |
| Figure 4.15: Current –Voltage characteristics of G-SiO ₂ samples S3 at different temperature. | 69 |
| Figure 4.16: 0.07 M whitish ZnCl ₂ solution | 70 |
| Figure 4.17: Initial 0.07 M ZnCl ₂ solution (a) and same solution after adding G-SiO ₂ (b) | 71 |
| Figure 4.18: 0.07 M ZnCl ₂ solution and G-SiO ₂ after one hour(c) and six hours(d) | 71 |
| Figure 4.19: 0.07 M ZnCl ₂ solution and G-SiO ₂ after six days (e) and after filtering (f) | 72 |
| Figure 4.20: CV measurement to check the redox peak of Zn ion in the water. | 72 |
| Figure 4.21: Reduction of the redox peak with respect to time. | 74 |
| Figure 4.22: Adsorption of 0.07 M ZnCl ₂ by G-SiO ₂ | 75 |
| Figure 4.23: G-SiO ₂ sample collected after filtering the solution | 75 |
| Figure 4.24: EDS of the filtered G-SiO ₂ which shows Zn in the material. | 76 |

Figure 4.25: EDS of the filtered G-SiO₂ which is washed with deionized water

77

Figure 4.26: Adsorption of 0.02 M ZnCl₂ by G-SiO₂

79

Abstract

This thesis consists of two research problems in the water decontamination area. In the first work, the main focus is to understand the structure and photocatalytic activity of titanium dioxide with graphene (G-TiO₂) which is synthesized by using sol-gel method. The photocatalytic activity of TiO₂ is limited by the short electron hole pair recombination time. Graphene, with high specific surface area and unique electronic properties, can be used as a good support for TiO₂ to enhance the photocatalytic activity. The obtained G-TiO₂ photocatalysts has been characterized by X-Ray Diffraction (XRD), Raman Spectroscopy, Transmission Electron Microscopy (TEM), FTIR Spectroscopy and Ultraviolet visible (UV-vis) Spectroscopy. This prepared G-TiO₂ nanocomposite exhibited excellent photocatalysis degradation on methyl orange (MO) under irradiation of simulated sunlight. Such enthralling photocatalyst may find substantial applications in various fields.

The primary objective of the second work is to understand the nanocomposite structure of SiO₂ coated over graphene (G) nanoplatelets. An attempt has been made to synthesize G-SiO₂ nanocomposite using sol-gel technique. The G-SiO₂ nanocomposite is characterized using Scanning Electron Microscopy (SEM), Transmission Electron Microscopy (TEM), Raman spectroscopy, FTIR spectroscopy, and Electrochemical and Electrical measurement technique, respectively. In this work, G-SiO₂ nanoparticles with the water containing salts of zinc is added, and allowed to settle in water. The ZnCl₂

concentration displays a whitish color solution which has turned to colorless within one or two hours of treatment with G-SiO₂ nanocomposites. The presence of heavy metal is tested using electrochemical cyclic voltammetry (CV) technique. The CV measurement on the water treated with G-SiO₂ has been tested for several days to understand the presence of heavy metals in water. Interestingly, the near complete separation has been observed by treating the heavy metal contaminated water sample for one to two days in presence of G-SiO₂ nanoparticles. The redox potential observed for the heavy metal has been found to diminish as a function of treatment with respect to time, and no redox peak is observed after the treatment for four to five days. Further test using EDS measurement indicates that the heavy metal ions are observed within the G-SiO₂ nanocomposite. The recovery of G-SiO₂ nanocomposite is obtained by washing using deionized water. Our experimental finding indicates that the G-SiO₂ nanocomposite could be exploited for potential heavy metals cleaning from waste or drinking water.

Chapter 1

Introduction

1.1 Overview of Nanocomposite Materials

Nanotechnology can be defined as the manipulation, manufacture, characterization, and application of material science and engineering and devices on the scale of atoms or small groups of atoms [1-4]. Some defined nanotechnology as the understanding and control of matter at the nanoscale where this material exhibits unique physical and chemical properties and novel applications [5]. The “nanoscale” is typically measured in nanometers, or billionths of a meter. One nanometer (nm) is equal to the width of 6 carbon atoms or 10 water molecules. A red blood cell is approximately 7000 nm wide. So nanocomposite materials can be defined as the nanoscale materials which have unique physical and chemical properties with novel applications.

The prefix “nano” comes from the Greek word for “dwarf” [6]. Nanoparticles play a fascinating role in chemical transformation. Nanomaterials are much more reactive as they have larger surface to volume ratio compared to the bulk mineral. There are two major classes of nanomaterials are environmental (metal oxides and metal sulfides commonly found as minerals) and engineered. Synthetically manufactured nanoparticles are called engineered nanoparticles. Recently, four different types of engineered nanoparticles are being investigated for their excellent property. They are carbon based (fullerene, nanotube, and graphene), metal based (metal oxides, quantum dots, nanogold,

and nanosilver), dendimers (constructed from pieces of different nanomolecules called nanopolymers) and composites (mixtures of nanoparticles or nanoparticles attached to larger, bulk-materials) [8]. These nanomaterials play an important role in the society. These particles receive much of the interest of the researchers and funding

1.1.1 Overview of Graphene

In 1962, Hanns-Peter Boehm was first to give the concept of single layer carbon foil [9]. But Andre Geim and Konstantin Novoselov are the pioneers who discovered the graphene, the monolayer material. Later in 2010, both got the Noble Prize in physics for this spellbinding material.

Graphene is the buzz word of new era is nothing but a Sp^2 bonded allotrope of carbon which has densely packed honeycomb lattices structure. Graphene, two dimensional allotrope of carbon [10] has attracted much attention due to its exciting structural [11], electrochemical [12], physicochemical and electronic properties [13]. It shows high thermal conductivity ($5000 \text{ W m}^{-1} \text{ K}^{-1}$) [14], excellent mobility of charge carriers ($200\,000 \text{ cm}^2 \text{ V}^{-1} \text{ s}^{-1}$) [15].

Activated carbon or activated charcoal is extremely porous material that gives it a large surface area [9]. This makes it suitable for adsorption process. In adsorption process, a solid is used for removing a soluble substance from the water. Activated carbon is the ideal material for adsorption.

Carbon nanotubes prove itself as a good adsorbent by removing several heavy metal ions such as lead, cadmium, chromium, copper, and nickel from wastewater [16-19]. From table 1.1 it is observed that carbon nanotube and graphene has

some similar properties and according to some researcher graphene can be a good adsorbing material as it has larger surface area in between the graphene flakes [20].

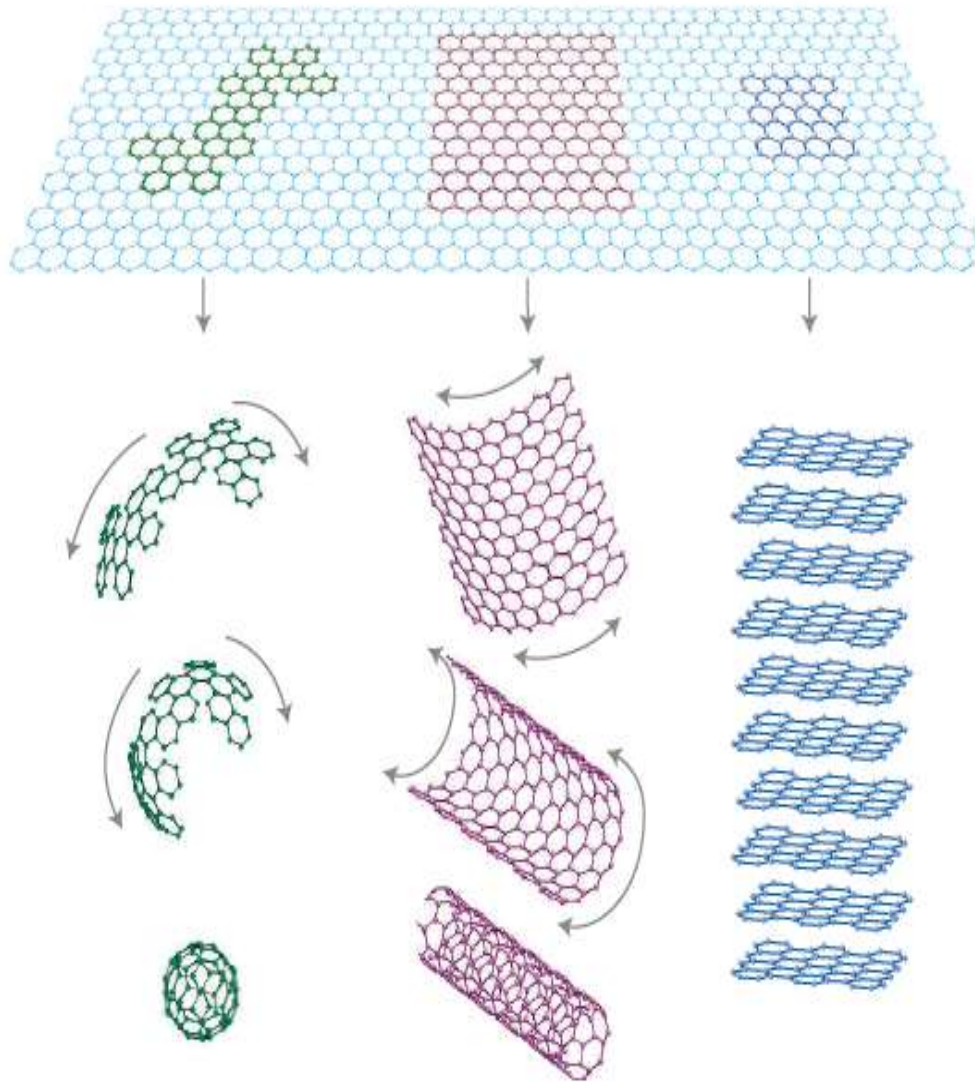


Figure 1.1: Mother of all graphitic forms. Graphene is a building block for all carbon materials allotropes. It can be wrapped up into 0D buckyballs, rolled into 1D nanotubes or stacked into 3D graphite [21]

Table 1.1: Comparison between different allotropes of carbon: [9]

| | Diamond | Graphite | C ₆₀ | Carbon nanotube | Graphene |
|-----------------------|-----------------------------|---------------------------------|---------------------------------|---------------------------------|------------------------------|
| Color | Colorless | Steel black to grey | Black solid | Black | Black |
| Density | 3.52 g/cm ³ | 1.99-2.3 g/cm ³ | 1.7-1.9 g/cm ³ | 2 g/cm ³ | >1 g/cm ³ |
| Electric conductivity | Insulator | Conductor | Semi-conductor | Conductor to semi-conductor | Conductor to semi-conductor |
| Hybridization | sp ³ tetrahedral | sp ² trigonal planar | sp ² trigonal planar | sp ² trigonal planar | Sp ² planer sheet |
| Crystal Structure | Cubic | Tabular | Truncated icosahedron | Cylindrical | Honeycomb |

1.1.2 Overview of Metal Oxides

1.1.2.1 Titanium Dioxide

Titanium dioxide is also known as titanium (iv) oxide or titania. Naturally occurred titanium dioxide has three mineral compounds. They are known as anatase, brookite, and rutile [22]. It has wide range of application in different industries such as white pigment industry as it is one of the whitest materials exists on the earth and it has very high refraction properties. It contributes to increase the brightness of toothpaste and

some medications. However, it is also used as photovoltaic devices [23], sensors [24], as a food additive [25], in cosmetics [26] and as a potential tool in cancer treatment [27]. It has application in the field of photocatalysis also.

1.1.2.1 Silicon Dioxide

Silicon dioxide, the most abundant material in the world is also known as silica. Silica can be found in different forms such as sand, quartz, sandstone, and granite. Silica is used primarily in the production of glass, optical fibers for telecommunications, whiteware ceramics (earthenware, stoneware, and porcelain) Silica is used as a desiccant [9]. It is the soul material for the semiconductor industry as it has good thermal and dielectric property. It is reported that iron (III) oxide/silica based nanomaterial is used as an adsorbent to remove the arsenic from water [28]. Silicon dioxide also used as the supporting material of titanium dioxide to enhance the photocatalytic activity.

In this research, Graphene (G) based metal oxides such as Graphene with titanium dioxide (G-TiO₂) and graphene with silicon (G-SiO₂) are synthesized, characterized by using different characterization techniques and employed them as photocatalyst and adsorbent, respectively.

1.2 Applications of Nanocomposite Materials

Nanocomposite materials has shown huge potential in areas of daily goods, information and communication technologies, medical care and water decontamination. It is possible with the nanomaterials to achieve the desired property by manipulating the

structures of materials at the nanoscale. Some of the daily used nanomaterial based examples are:

Some nanoscale additives are used in baseball bats, helmets, automobile bumpers, and tennis racket. Nanoscale additives are also used for surface treatment. These materials are used in daily cosmetic products like, creams, lotions, shampoos, and specialized makeup. These additives are useful to make the products lightweight, stiff, and resilient Nanostructured ceramic coatings challenge the existence of conventional wear-resistant coatings by showing high toughness. Even in automotive products, rechargeable battery systems; tires and also in the food industry are using nanomaterials. Nanotechnologies are getting more and more popular in many computing, communications, and other electronics applications. With the aid of these nanomaterials, it is possible to provide faster, smaller, and more portable systems that can handle and store larger and larger amounts of data [5, 29-30].

Nanoscale transistors have shown us the dream of more powerful, energy efficient, fast computers. In few decades, it will be possible to store entire memory on a single tiny chip. Magnetic random access memory (MRAM), with the aid of nanometer-scale magnetic tunnel junctions, can save even enciphered data during a system shutdown or airplane crash. Nanostructured polymer films known as organic light-emitting diodes screens take the displays of TVs, laptop computers, and other devices to a new dimension. It provides clear and distinct image, high angles, and use low power to run [5,29-30].

Nanotechnology plays an important role in the field of nanomedicine. Engineered nanodevices and nanostructures are used for monitoring, repair, construction, and control

of human biological systems at the molecular level [2, 7, 31-33]. One of the key purposes served by the nanotechnology and the nanomaterials are proper distribution of drugs within the patient's body [33-36]. At present, lots of people die for cardiac diseases. To diagnosis, imaging, and tissue engineering to treat the cardiovascular diseases different types of nanomaterials and nanotechnology-based tools are being used [37]. Nanomaterials have bright future in nanodentistry. With the aid of nanomaterials and nanorobotics it is possible to maintain near-perfect oral health [7, 38-40].

The recent development of nanotechnology has opened the window in the area of water decontamination through several nanomaterials, processes, and tools. Today nanoparticles, nanomembrane and nanopowder are used for detection and removal of chemical and biological substances include metals (Cadmium, copper, lead, mercury, nickel, zinc), nutrients (Phosphate, ammonia, nitrate and nitrite), cyanide, organics, algae (cyanobacterial toxins) viruses, bacteria, parasites and antibiotics [41].

1.3 Water Decontamination Process

Water is one of the essential parts of human life. Advancement of technology, rapid growth of industries, and population problem are the main reasons of water pollution. Due to the scarcity of the pure water, lots of diseases and health issues encounter in our daily life. There are lots of processes adopted by the human kind for hundreds of years. Recently, nanomaterials are getting popularity in the field of water decontamination. Few advantages and disadvantages of conventional technologies are discussed in table 1.2.

Table 1.2 Review of conventional technologies employed for water purification [42]

| Technology used | Advantages | Disadvantages |
|----------------------------|---|---|
| Reverse osmosis | Removes TDS, heavy metals, fluoride, pesticides, micro-organisms | -Low recovery -High maintenance cost -Pretreatment needed |
| Grannular activated carbon | -Removes VOCs, pesticides, excess chlorine, color, odor -High throughput | Doesn't remove: organic pollution, TDS, nitrates, fluorides, hardness -Expensive |
| UV-based filtration | -Broad-range micro-organism removal -High filtration capacity | -Effectively degrades only micro-organisms -High costs |
| Electro-dialysis | High TDS removal efficiency | -Proportional increase in cost with TDS -Doesn't remove: micro-organisms |

Table 1.3 Advantage and disadvantages of different heavy metal removal techniques [43]

| Technique used | Advantage | Disadvantage |
|--------------------------|--|---|
| chemical precipitation | -Simple process - low capital cost | ineffective when metal ion concentration is low |
| Ion exchange | Can be regenerated | -Chemical reagents cause serious secondary pollution -Expensive |
| Adsorption process | Very efficient for low concentration of waste containing heavy metal | -High cost of activated carbon Efficiency depends on type of adsorbent |
| Membrane filtration | High efficiency | -High cost -Complex process -Membrane fouling |
| Coagulation-flocculation | good sludge settling and dewatering characteristics | involves chemical consumption and increased sludge volume generation. |
| Flotation | -high metal selectivity, -high removal efficiency, -high overflow rates, -low detention periods, -low operating cost | -high initial capital cost, -high maintenance |

In the present research, main focus will be on photocatalysis and adsorption process. G-TiO₂ and G-TiO₂ be employed as photocatalyst and adsorbent, respectively.

1.4 Photocatalysis

For last 10-15 years extensive research was performed on photocatalysis of TiO₂. In this process, when UV irradiation equal or more then the band gap impinge upon the TiO₂, electrons from valance band get excited and move to the conduction band, hence form electron and hole pairs. These holes oxidize the H₂O and generate OH* radicals and the electron is responsible for the reduction process on the TiO₂ surface [44]. This OH* then react with the organic materials and produce CO₂ and H₂O.

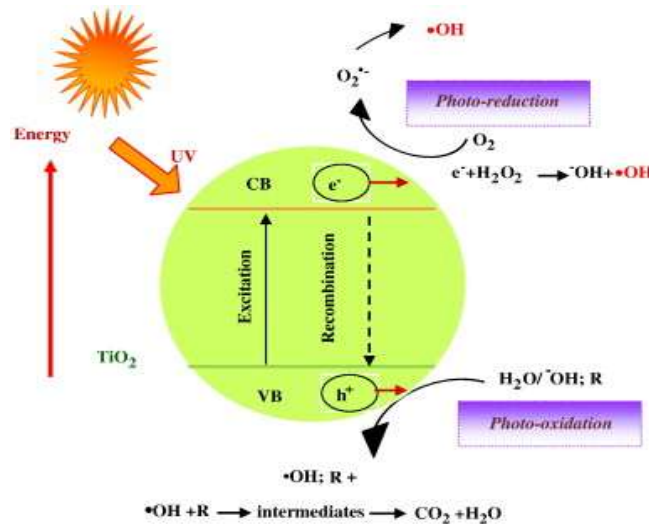


Figure 1.2: Mechanism of the photocatalytic effect of TiO₂ [45]

1.5 Adsorption

In adsorption process, a solid is used for removing a soluble substance from the water. In this process, molecules of the adsorbate are attracted to and conglomerate on the surface of the adsorbent [46]. This is one of the efficient and economic methods for removing heavy metal from water and works well when the concentration of the heavy metal is low in the water. Design and operation process is flexible for the adsorption process. In addition, adsorbents can be regenerated by suitable desorption process [43].

1.6 Research Aims

To investigate the structure of a new generation nanomaterial and to develop a photocatalyst for the remediation of organic effluents from water. To find the possibility of developing an efficient nanostructured adsorbent for the remove heavy metals from water.

1.6.1 Overall Objective of the Study

- a) To synthesis and understand the characteristics of newly developed G-TiO₂ by using different characterization techniques.
- b) To employ G-TiO₂ as a photocatalysts to remove organic material from water and also compare the effectiveness of this photocatalysts with commercially available p25.
- c) To synthesis and understand the characteristics of newly developed G-SiO₂ by using different characterization techniques.

- d) To employ G-SiO₂ as an adsorbent to remove heavy metal from water. In this study, Zn has been taken as the adsorbate.

Chapter 2 corresponds to the discussion of important techniques used to characterize the synthesized Graphene Metal Oxide nanocomposites.

Chapter 3 provides the synthesis procedure of G-TiO₂ nanoparticles for photodegradation activity. The results obtained from different characterization techniques and possible application of G-TiO₂ as a photocatalyst for remediation of Methyl Orange from water gets the primary focus of this section. Photodegradation capability of the G-TiO₂ also compared with commercially available P25.

Chapter 4 provides the synthesis procedure of G-SiO₂ nanoparticles for adsorption process. This chapter discusses the results obtained from different characterization techniques. Application of G-SiO₂ as an adsorbent to remove the Zn ions from water gets the main concern in this section.

Finally, chapter 5 provides the conclusion based on the experimental results and recommendation for the future work with G-TiO₂ and G-SiO₂ as photocatalyst and adsorbent, respectively.

1.7 References

- [1] Internet website: <http://www.britannica.com>
- [2] Emerich DF, Thanos CG. Nanotechnology and medicine. *Expert Opin Biol Ther* 2003;3:655 - 63 M.
- [3] Sahoo SK, Labhasetwar V. Nanotech approaches to drug delivery and imaging. *Drug Discov Today* 2003;8:1112- 20
- [4] M. Matsudai and G. Hunt, Nanotechnology and public health. *Nippon Koshu Eisei Zasshi*, 2005, 52, pp. 923–927

- [5] Internet website: <http://www.nano.gov/>
- [6] Whitesides GM. The dright T size in nanobiotechnology. *Nat Biotechnol* 2003;21:1161- 5.
- [7] S.K. Sahoo, S. Parveen, and J.J. Panda, The present and future of nanotechnology in human health care. *Nanomedicine: Nanotechnology, Biology and Medicine*, Volume 3, Issue 1, March 2007, pp. 20–31.
- [8] Richard M. DiSalvo, Jr., PE Gary R. McCollum, Evaluating The Impact Of Nanoparticles On Wastewater Collection And Treatment Systems In Virginia, WATER JAM 2008 Virginia Beach, Virginia September 7-September 11, 2008
- [9] Internet website: <http://en.wikipedia.org/>
- [10] K.S. Novoselov, A.K. Geim, S.V. Morozov, D. Jiang, Y.Zhang, S.V. Dubonos, I.V. Grigorieva, A.A. Firsov, *Science* 306 (2004) 666.
- [11] J. C. Meyer, A. K. Geim, M. I. Katsnelson, K. S. Novoselov, T. J. Booth, and S. Roth, “The structure of suspended graphene sheets,” *Nature*, vol. 446, no. 7131, pp. 60-63, Mar. 2007.
- [12] H.-P. Huang and J.-J. Zhu, “Preparation of Novel Carbon-based Nanomaterial of Graphene and Its Applications Electrochemistry,” *Chinese Journal of Analytical Chemistry*, vol. 39, no. 7, pp. 963-971, Jul. 2011.
- [13] A. H. C. Neto, F. Guinea, N. M. R. Peres, K. S. Novoselov, and A. K. Geim, “The electronic properties of graphene,” arXiv:0709.1163, Sep. 2007.
- [14] A. A. Balandin, S. Ghosh, W. Z. Bao, I. Calizo, D. Teweldebrhan, F. Miao and C. N. Lau, *Nano Lett.*, 2008, 8, 902–907.
- [15] K. I. Bolotin, K. J. Sikes, Z. Jiang, M. Klima, G. Fudenberg, J. Hone, P. Kim and H. L. Stormer, *Solid State Commun.*, 2008, 146, 351–355.
- [16] Wang, H.J., Zhou, A.L., Peng, F., Yu, H., Yang, J., Mechanism study on adsorption of acidified multiwalled carbon nanotubes to Pb(II). *J. Colloid Interface* 2007a *Sci.* 316, 277-283.
- [17] Kuo, C.Y., Lin, H.Y., Adsorption of aqueous cadmium (II) onto modified multiwalled carbon nanotubes following microwave/chemical treatment. *Desalination* 2009.249, 792-796

- [18] Pillay, K., Cukrowska, E.M., Coville, N.J., Multi-walled carbon nanotubes as adsorbents for the removal of parts per billion levels of hexavalent chromium from aqueous solution. *J. Hazard. Mater* 2009. 166, 1067-1075.
- [19] Kandah, M.I., Meunier, J.L., Removal of nickel ions from water by multi-walled carbon nanotubes. *J. Hazard. Mater.* 2007.146, 283-288
- [20] Liu Q, Shi J, Zeng L, Wang T, Cai Y, Jiang G. *J Chromatogr A*. Evaluation of graphene as an advantageous adsorbent for solid-phase extraction with chlorophenols as model analytes. 2011 Jan 14;1218(2):197-204. Epub 2010 Nov 19
- [21] A.K. Geim, K.S. Novoselov, *Nat. Mater.* 6 (2007) 183.
- [22] Internet website: <http://www.wisegeek.com>
- [23] Kalyanasendevan, K.; Gratzel, M.; in *Optoelectronics Properties of Inorganic Compounds*; p. 169-194; Roundhill, D.M.; Fackler, J.P. (Editors); Plenum, New York, 1999.
- [24] Sheveglieri, G. (Editor); *Gas sensors*; Kluwer, Dordrecht, 1992.
- [25] Phillips, L.G.; Barbeno, D.M.; *J. Dairy Sci.* 1997, 80, 2726.
- [26] Selhofer, H.; *Vacuum Thin Films* (August, 1999) 15.
- [27] Fujishima, A.; Rao, T.N.; Tryk, D.A.; *J. Photochem. Photobiol. C: Photochem. Rev.* 2000, 1, 1.
- [28] Le Zeng, *Arsenic Adsorption from Aqueous Solutions on an Fe(III)-Si Binary Oxide Adsorbent*, *Water Qual. Res. J. Canada*, 2004 • Volume 39, No. 3, 267–275.
- [29] Internet website: <http://www.azom.com>
- [30] Internet website: <http://www.nanocompositech.com>
- [31] Moghimi SM, Hunter AC, Murray JC. *Nanomedicine: current status and future prospects.* *FASEB J* 2005;19:311 - 30.
- [32] Emerich DF. *Nanomedicine—prospective therapeutic and diagnostic applications.* *Expert Opin Biol Ther* 2005;5:1 - 5.
- [33] Jain KK. *Nanodiagnostics: application of nanotechnology in molecular diagnostics.* *Expert Rev Mol Diagn* 2003;3:153 - 61.

- [34] Shaffer C. Nanomedicine transforms drug delivery. *Drug Discov Today* 2005;10:1581- 2.
- [35] Freitas Jr RA. What is nanomedicine? *Dis Mon* 2005;51:325- 41.
- [36] Labhasetwar V. Nanotechnology for drug and gene therapy: the importance of understanding molecular mechanisms of delivery. *Curr Opin Biotechnol* 2005;16:674 - 80.
- [37] Wickline SA, Neubauer AM, Winter P, Caruthers S, Lanza G. Applications of nanotechnology to atherosclerosis, thrombosis, and vascular biology. *Arterioscler Thromb Vasc Biol* 2006;26: 435- 41.
- [38] West JL, Halas NJ. Applications of nanotechnology to biotechnology commentary. *Curr Opin Biotechnol* 2000;11:215 - 7.
- [39] Shi H, Tsai WB, Garrison MD, Ferrari S, Ratner BD. Templateimprinted nanostructured surfaces for protein recognition. *Nature* 1999;398:593- 7.
- [40] M.F. Ashby, P.J. Ferreira, and D.L. Schodek, *Nanomaterials and nanotechnologies in health and the environment. Nanomaterials, Nanotechnologies and Design*, 2009, pp. 467–500.
- [41] Dhermendra K. Tiwari, J. Behari and Prasenjit Sen Application of Nanoparticles in Waste Water Treatment, *World Applied Sciences Journal* 3 (3): 417 433, 2008
- [42] T. Pradeep, Anshup, Noble metal nanoparticles for water purification: A critical review *Thin Solid Films* 517 (2009) 6441–6478
- [43] Fenglian Fu a, Qi Wang, Removal of heavy metal ions from wastewaters: A review *Journal of Environmental Management* 92 (2011) 407-418
- [44] Manoj K. Ram and Ashok Kumar Decontamination Using Nanotechnology, Book Chapter 1
- [45] Ahmed, S., Rasul, M.G., Martens, W.N., Brown, R.J., & Hashib, M.A. (2010) Heterogeneous photocatalytic degradation of phenols in wastewater : a review on current status and developments. *Desalination*, 261(1-2), pp. 3-18
- [46] Internet website: <http://www.carbtrol.com>

Chapter 2

Characterization Tools

Characterization can be described as the external techniques to investigate the internal features like composition and structure (including defects) of a material that are significant for particular preparation, study of properties, or use, and suffice for reproduction of the materials [1-2]. This chapter reviews the techniques used for characterization of G-TiO₂ and G-SiO₂.

2.1 Raman Spectroscopy

Raman spectroscopy is a non-contact and non-destructive analysis to identify the molecules and study their structural properties [3]. Raman spectroscopy can be used to study three different phases of samples. This process provides information about vibrational, rotational and other low frequency transitions in molecules. In this technique, a laser source is used as monochromatic light source which is absorbed by the sample and then reemitted. Shift from the original monochromatic frequency with the reemitted frequency of light is called the Raman Effect. This effect is discovered in 1928 by Chandrasekhara Venkata Raman [1, 4].



Figure 2.1: Renishaw Raman Spectrometer at USF

The commercially available Raman spectrometer has five main components. Continuous wave laser like Ar⁺ at a wavelength of 514.5 nm, sample illumination and scattered light collection system, sample holder, monochromator or spectrograph and detection system.

2.2 Scanning Electron Microscopy (SEM)

The scanning electron microscope (SEM) uses electron instead of light and produces high resolution images of high magnification. From tungsten cathode, electrons are thermionically emitted or emitted via field emission and move towards the anode through electromagnetic fields and lenses and the beams are focused down towards the sample in a vertical vacuum chamber. When the beams hit the sample, electrons and X-rays are ejected from it. The detectors collect these electrons and convert them into

signals. The signal is then transmitted to a television like screen to produce the final image [1, 5].

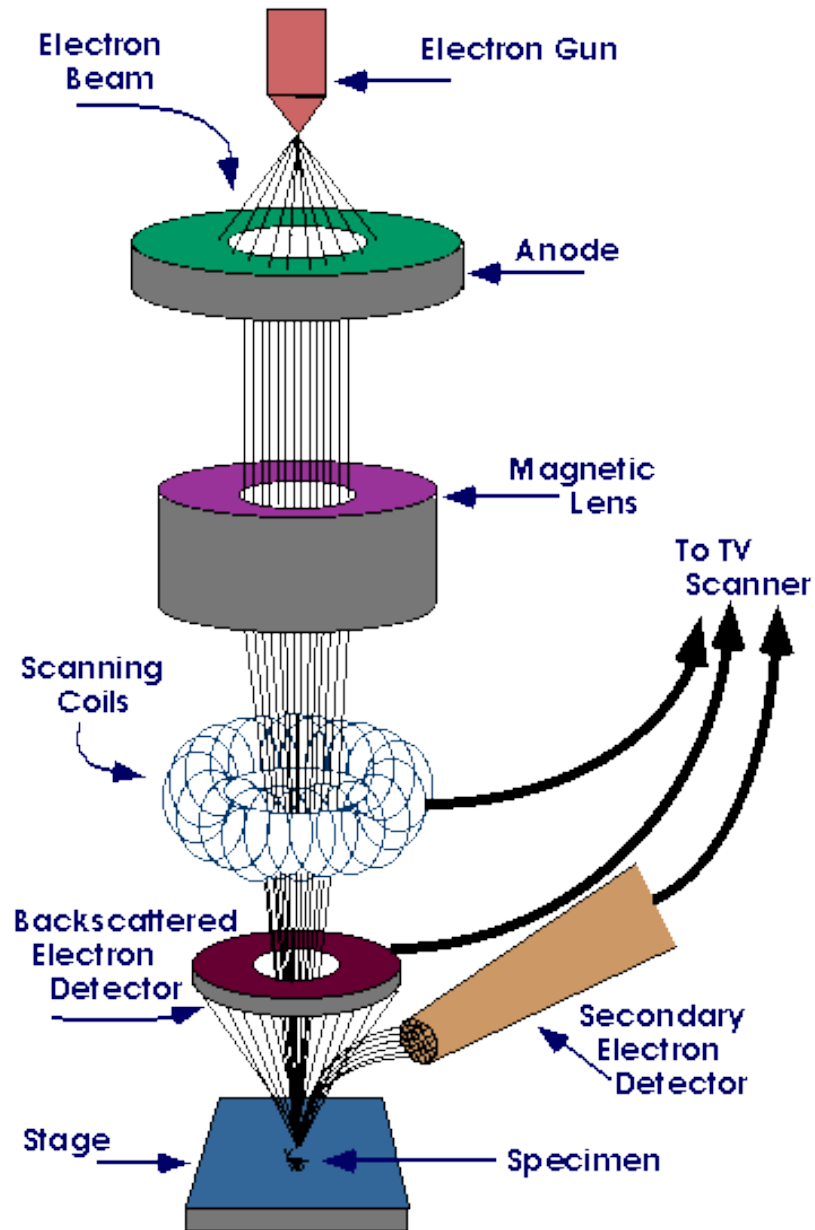


Figure 2.2: Shows the basic block diagram of a Scanning Electron Microscope.

(Diagram courtesy of Iowa State University) [5]

2.3 Energy Dispersive Spectroscopy (EDS)

EDS measures the energy and intensity (or counts) of the characteristic X-rays (and background continuum) to identify the elements in the sample. The three main parts of the EDS are: the detector, the processing electronics, and the MCA and display. The detector collects the x-rays after the electron beam hits the sample. The x-rays are characteristic of the quantity of each element present in the area scanned by the electron beam [6].



Figure 2.3: Scanning Electron Microscopy (SEM) and Energy Dispersive Spectroscopy (EDS) at USF

2.4 X-Ray Diffraction (XRD)

X-ray diffraction is a nondestructive technique, where shorter wavelength x-rays is produced. X-ray diffraction is used to know the crystallographic structure of the material. Typically, X-ray tube is maintained at the high voltage and the electrons move

towards the anode. As the electron hit the anode, X-rays are produced and radiate in all directions [7].

The relation by which diffraction occurs is known as the Bragg law or equation which is stated below:

$$n\lambda \sin\theta = 2d \quad (2.1)$$

Here, d is lattice interplanar spacing of the crystal, θ is X-ray incident angle, λ is wavelength of characteristic X-rays. Basic components of an X-ray diffractometer consist of a source of monochromatic radiation and an X-ray detector. Divergent slits are placed in between the X-ray source and the specimen and receiving slits are placed in between the specimen and the detector.[8]



Figure 2.4: X-Ray Diffraction machine at USF

2.5 Transmission Electron Microscope (TEM)

The Transmission Electron Microscope (TEM) and simple optical microscope both have the same basic principles. But in the case of TEM, it uses electrons instead of light. With TEM, it is possible to get thousand times better resolution than a light microscope [9]. In this technique, a beam of electrons interacts with the ultra-thin specimen as it passes through it. From the interaction of the transmitted electron beams and specimen, an image is created which is then magnified and focused onto an imaging device, such as a fluorescent screen [1, 6]. Objects of a few angstroms can be seen through TEM. Morphology and crystallographic information can be gathered from this machine as well [10].



Figure 2.5 Transmission Electron Microscope at USF

2.6 Fourier Transform Infrared Spectroscopy (FTIR)

Fourier Transform Infrared Spectroscopy (FTIR) is used to determine the chemical bonds and functional group. Each chemical bond in a molecule, absorb a certain wavelength of light. When infrared pass through the sample, it absorb some portion of infrared spectrum, which indicate the characteristic of the chemical bond. With the aid of this method unknown components can be detected. Analysis of different phases of sample can be done by this machine [11].

Different elements and different type of bonds vibrate several specific frequencies. Quantum mechanics indicates, these frequencies represent to the lowest frequency, E_0 and higher frequency, E_1 . By using absorb light energy on the bonds; the frequency of a molecular vibration can be increased. The difference between two energy states equals to energy of light absorbed [11].

$$E_1 - E_0 = (h c) / \lambda \quad (2.2)$$

Here, h corresponds to Planks constant

c corresponds to speed of light, and

λ corresponds to the wavelength of light.



Figure 2.6 Fourier Transform Infrared Spectroscopy at USF

2.7 UV-Visible Spectroscopy

In ultraviolet and visible (UV-Vis) absorption spectroscopy, a single wavelength or over an extended spectral range of light beam passes through a sample or reflects from a sample surface. Consequently, attenuation of the light is measured. Ultraviolet and visible light galvanize the outer electrons to higher energy levels [12].

UV-Vis spectroscopy is useful to characterize the absorption, transmission, and reflectivity of a variety of technologically important materials. UV-Vis spectroscopy is used for characterization of the optical or electronic properties of materials [12].



Figure 2.7: UV Visible Spectroscopy at USF

2.8 References

- [1] Internet website: <http://en.wikipedia.org/>
- [2] N. B. Hannay, Trace Characterization, ed. by W. W. Meinke and B. F. Scribner, NBS Monograph 100, U- S. Government Printing Office, Washington, D. C. (1967).
- [3] Internet website: <http://www.uku.fi>
- [4] Internet website: <http://www.princetoninstruments.com>
- [5] Internet website: <http://www.purdue.edu>
- [6] Internet website <http://www.nrec.usf.edu>
- [7] Internet website: <http://pubs.usgs.gov>
- [8] Internet website: <http://www.eserc.stonybrook.edu/>
- [9] Internet website: <http://www.nobelprize.org>

- [10] Internet website: <http://www.unl.edu>
- [11] Internet website: <http://www.wcaslab.com>
- [12] Internet website: <http://www.files.chem.vt.edu>

Chapter 3

Synthesis, Characterization of G-TiO₂ and Application in Organic Material Remediation

3.1 Introduction

Fujishima and Honda [1] first introduced TiO₂-based photochemical electrode for photolysis of water, since then TiO₂ semiconductor has been considered as one of the best photocatalytic materials and studied extensively for the photodegradation of organic pollutants [2-4]. When sufficient UV irradiation falls upon the TiO₂, electrons got excited and move from valence band to the conduction band, thus form electron-hole pairs. These holes oxidize the H₂O and generate OH* radicals and the electron is responsible for the reduction process on the TiO₂ surface [5]. However, recombination time of electrons and holes in TiO₂ is much more rapid than the time of chemical interaction of TiO₂ with the adsorbed contaminants, which diminishes the efficiency of the photocatalytic activity [6-8]. Development of various nanocomposites such as TiO₂-Au composite [9], CdS/CdSe-TiO₂ hybrid [10-11], carbon nanomaterial doped TiO₂ [12-14], has promised to overcome this limitation and to obtain better photoresponse. Among those carbon nanotube (CNT)-TiO₂ nanocomposites [14-18] shows significant photocatalytic activity though CNT has some limitations [19-20].

Recently, graphene [21] has attracted much attention due to exciting structural [22], electrochemical [23], physicochemical and electronic properties [24]. It shows high

thermal conductivity ($5000 \text{ W m}^{-1} \text{ K}^{-1}$) [25], excellent mobility of charge carriers ($200000 \text{ cm}^2 \text{ V}^{-1} \text{ s}^{-1}$) [26]. Different studies of graphene-metal oxide indicate that graphene nanosheet could be a good electron carrier channel which indicates an effective supportive material [27]. Different properties of graphene intrigue us to synthesis G-TiO₂ nanocomposite to achieve higher photocatalytic response by delaying the electron hole recombination time.

This chapter discusses the synthesis procedure of G-TiO₂ nanoparticles for photodegradation activity. The results obtained from different characterization techniques and possible application of G-TiO₂ as a photocatalyst for remediation of Methyl Orange from water gets the primary focus of this section. Photodegradation capability of the G-TiO₂ also compared with commercially available P25

3.2 Materials for G-TiO₂

The hydrochloric acid (HCl), propanol and titanium (iv) isopropoxide are all A.C.S. grade, and purchased from Sigma–Aldrich (USA). The graphene platelets (less than 20 nm in thickness) were purchased from Angstrom Materials (USA). All the chemicals and materials were employed as purchased without any modifications unless and until discussed in the manuscript

3.3 Synthesis of G-TiO₂ Nanocomposite

The G-TiO₂ nanocomposite is synthesized in presence of graphene nanoplatelets in a solution mixture containing titanium (iv) isopropoxide and propanol solution. 0.19 gm of Graphene was dispersed in 20 mL of propanol after that 4 mL of titanium (iv)

isopropoxide was added into the dispersion. The mixture was stirred for 30 min at room temperature. Then 15 mL of deionized water and 0.5 mL HCl (1 M) was added dropwise and the reaction was stirred at 300 rpm for 24 hours at room temperature. The product was then centrifuged and washed with deionized water to remove any remaining organic residue. After that G-TiO₂ dried at 100 °C in a vacuum oven.

3.4 Flow Diagram of the Process

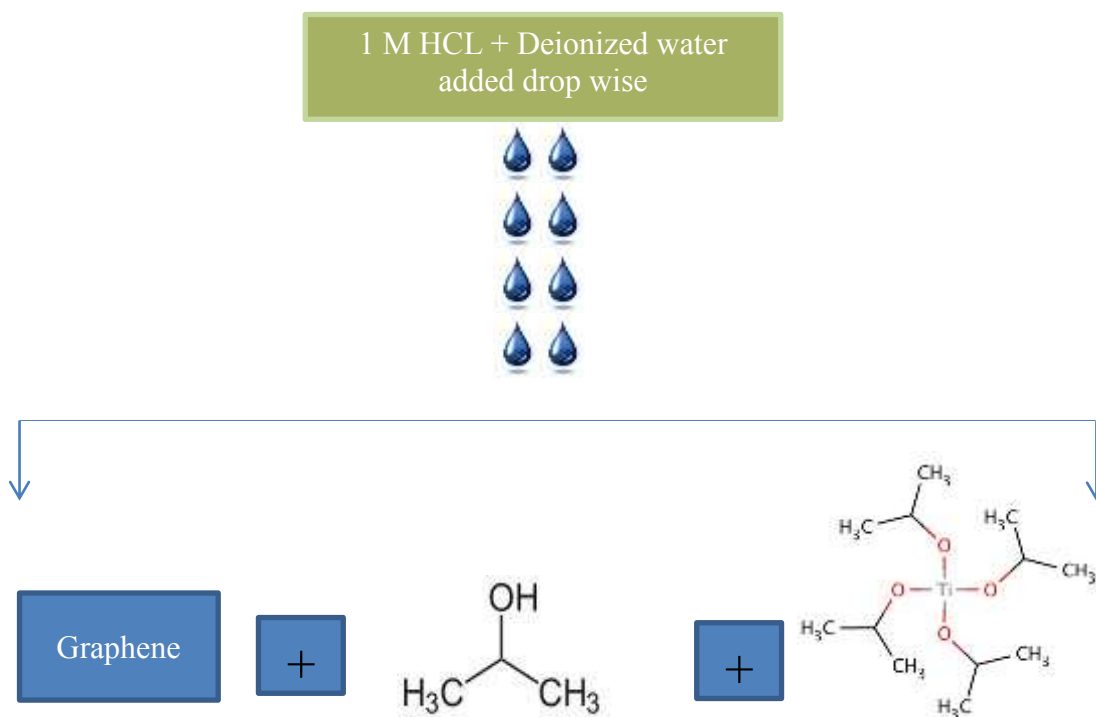


Figure 3.1 Flow diagram of G-TiO₂ Synthesis Process

3.5 Characterization of G-TiO₂

3.5.1 Machine Specification and Sample Preparation

The G-TiO₂ nanocomposite has been characterized by using Raman spectroscopy, Transmission Electron Microscope (TEM), Fourier Transform Infrared Spectroscopy (FTIR), powder X-Ray Diffraction (XRD), UV-visible Spectroscopy. Sample preparation methods for different instrument were different. Raman spectra of G-TiO₂ nanocomposite were measured using a Renishaw Raman Spectroscopy through a 514nm laser beam. Raman samples were prepared by adding a small amount of dry powder to ethanol and then the solutions were coated on silicon substrates by spin coating. The TEM measurements were done to investigate the morphology of the surface of the nanocomposite by using Technai F20. The TEM samples were prepared by adding a small amount of dry powder to ethanol, and a small drop of a solution was dropped on 300 mesh copper TEM grids for the measurement. FTIR spectra of nanocomposite was performed under transmission mode using KBr pellet under Perkin Elmer spectrometer. XRD analysis of G-TiO₂ samples were performed using X' Pert Pro system with Cu K α radiation ($\lambda = 1.54060\text{\AA}$) operated at 40 kV and 40 mA. For X-ray powder diffraction, samples were grinded well and put into the power holder. For UV-visible samples were coated on Si substrate and measured using Jasco V530 spectrometer.

3.5.2 Raman Spectroscopy

From figure 3.2, it has been observed that there are four peaks at low frequency region. They are assigned to the E_{1g} (176cm⁻¹), B_{1g} (446cm⁻¹), A_{1g} (552 cm⁻¹) and E_g (672cm⁻¹) modes of anatase phase respectively [28-29]. Like typical of graphene, D-

peak, G-peak and 2d-peak has been seen at 1390cm^{-1} , 1600 cm^{-1} and 2750cm^{-1} respectively [32-33].

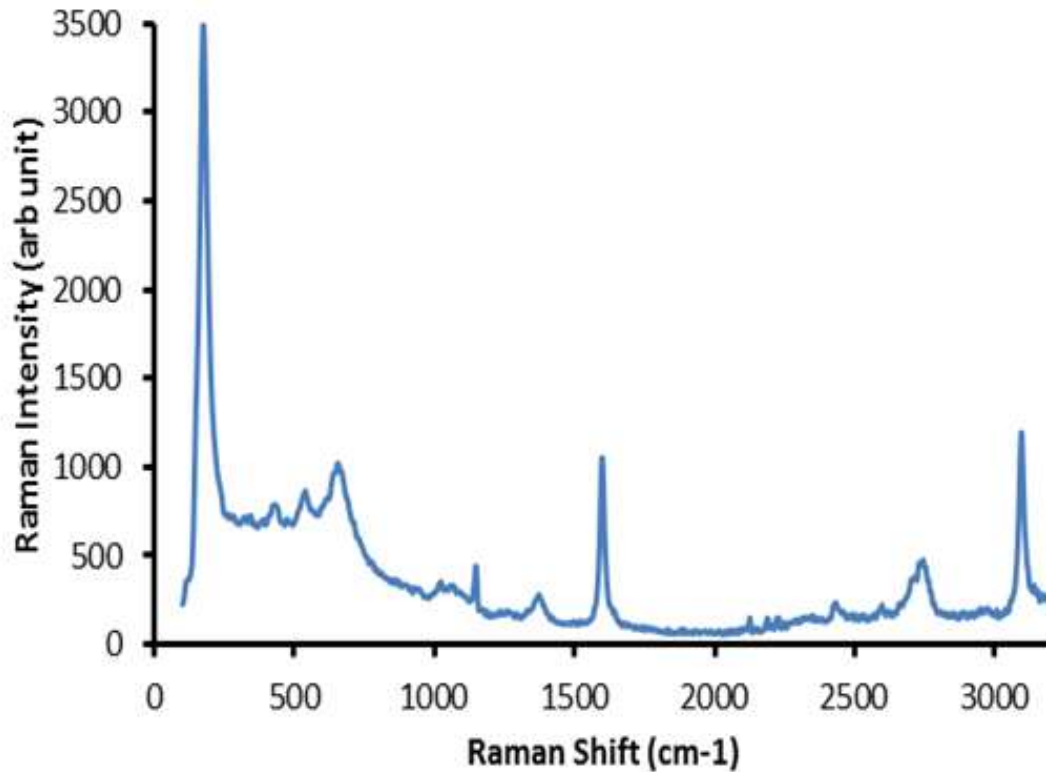


Figure 3.2: Raman spectra of G-TiO₂ nanocomposite.

3.5.3 Transmission Electron Microscopy

The morphology of the G-TiO₂ composite was characterized by TEM. Figure 3.3, 3.4, 3.5 and 3.6 show the TEM images of G-TiO₂ nanocomposite. Graphene sheets and spherical shaped nano structure of the TiO₂ nanoparticles can be clearly observed in the TEM images. It is observed that graphene sheets are covered with TiO₂ particles. The good distribution of TiO₂ particles and single layer structure of graphene will assist the photocatalysis [31].

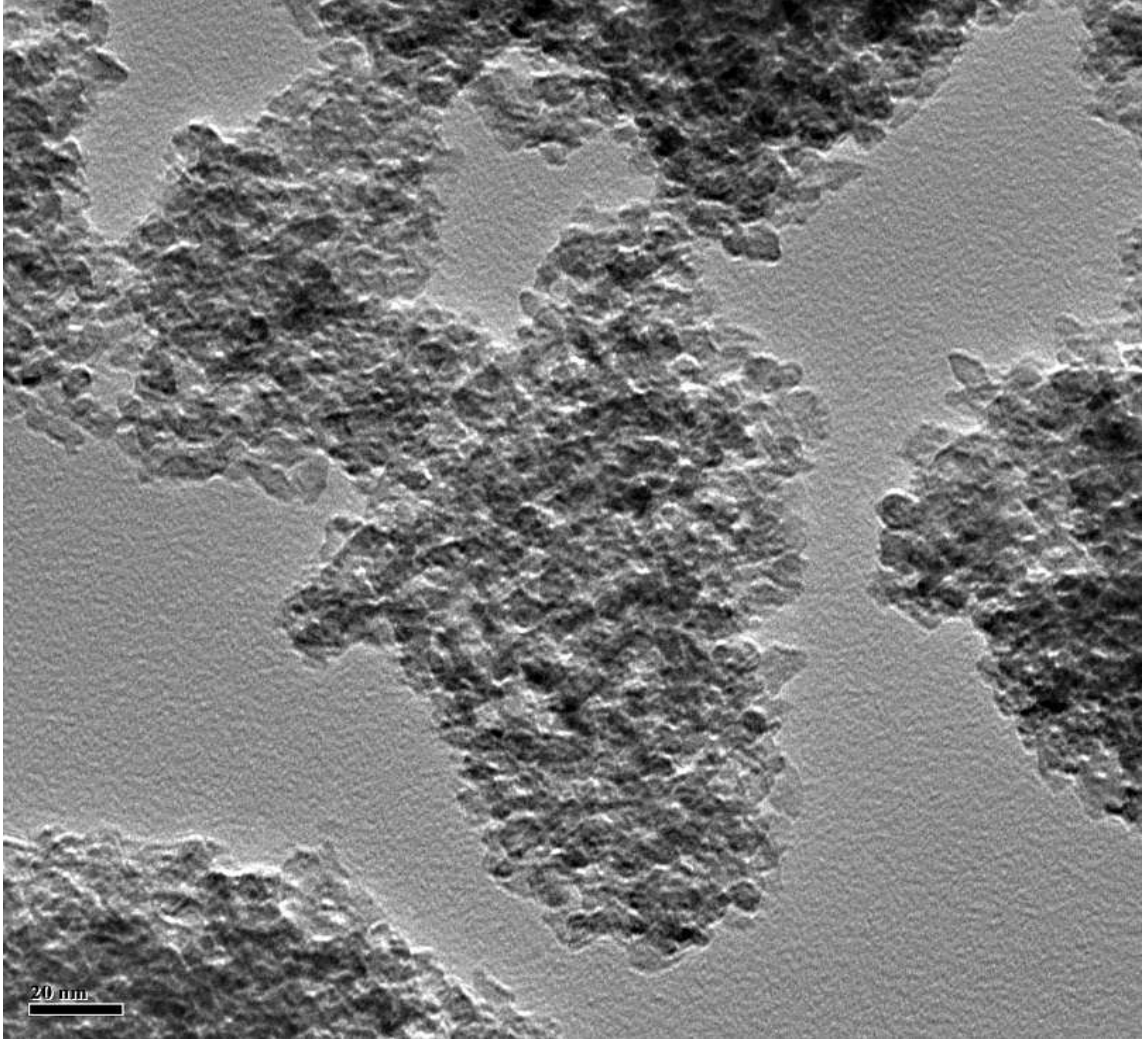


Figure 3.3: TEM image of G-TiO₂ (20 nm)

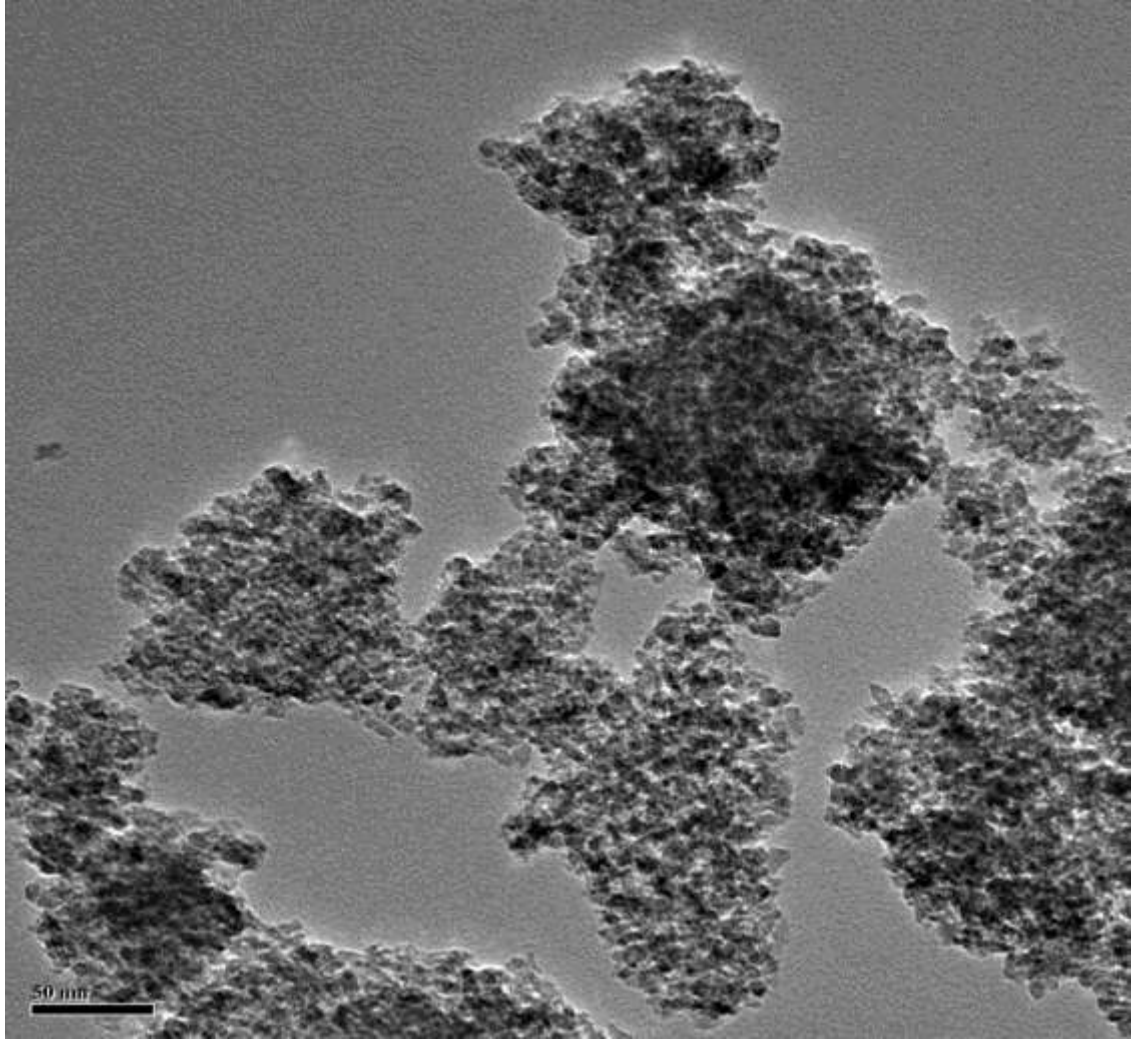


Figure 3.4: TEM image of G-TiO₂ (50 nm)

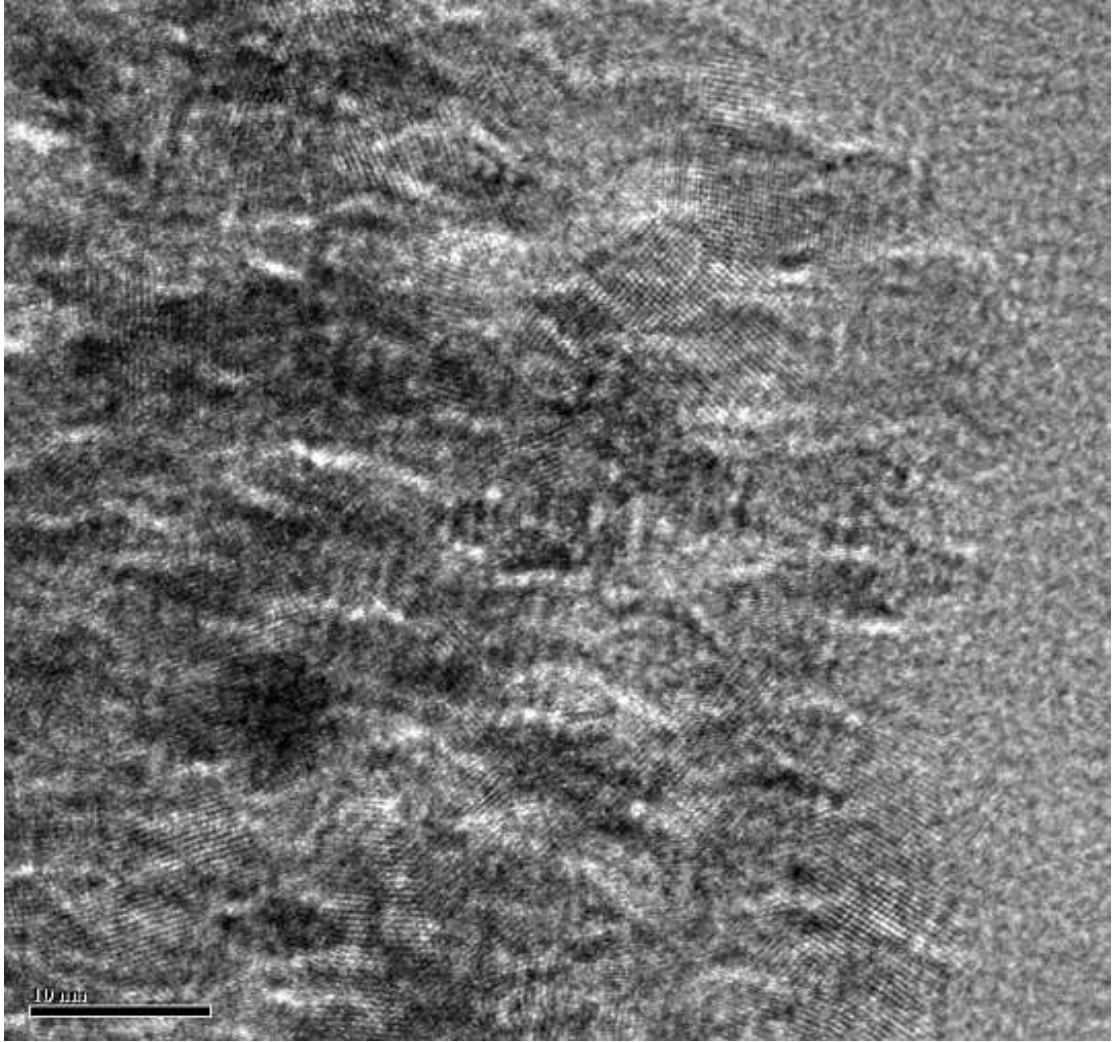


Figure 3.5: HRTEM image of G-TiO₂ (10 nm)

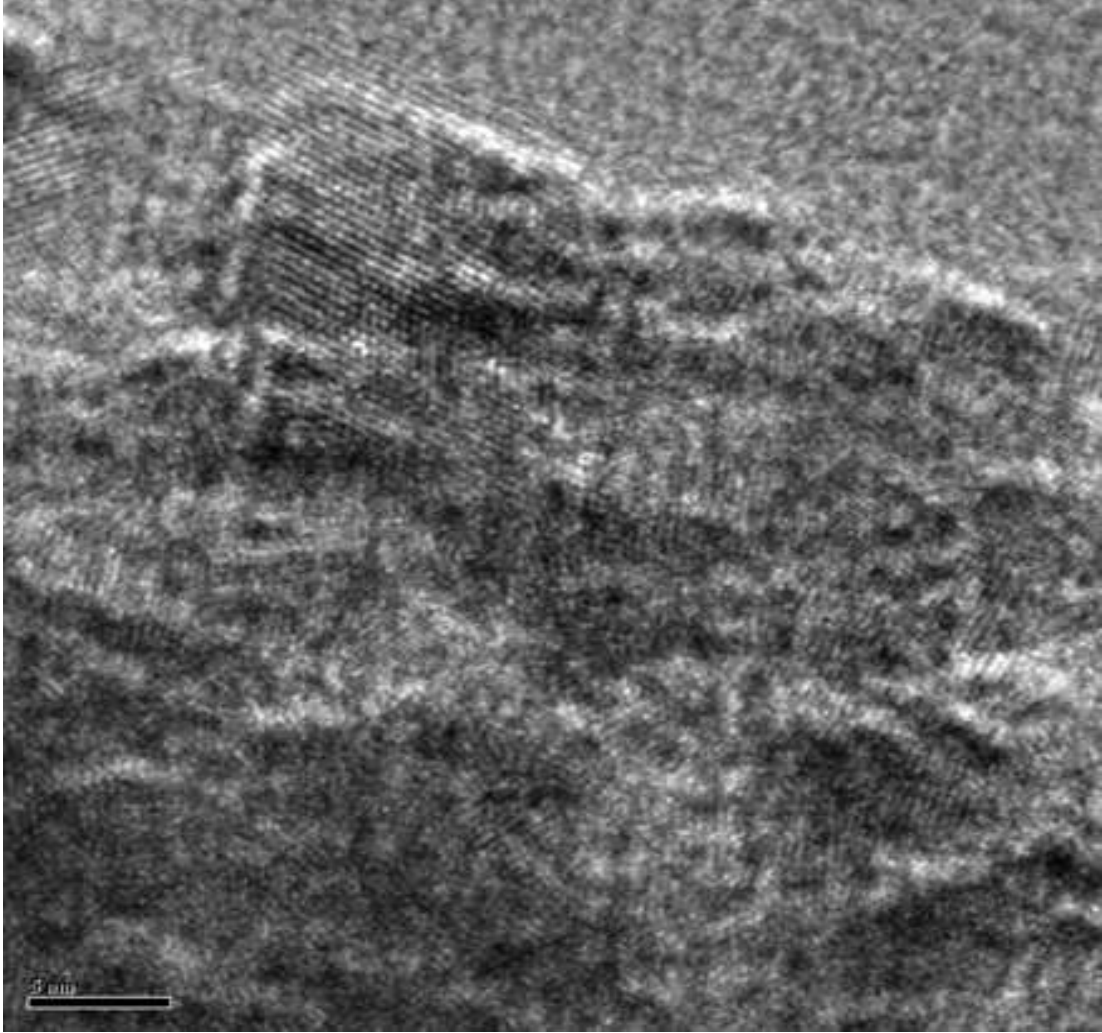


Figure 3.6: HRTEM image of G-TiO₂ (5 nm)

3.5.4 Fourier Transform Infrared (FTIR) Spectroscopy

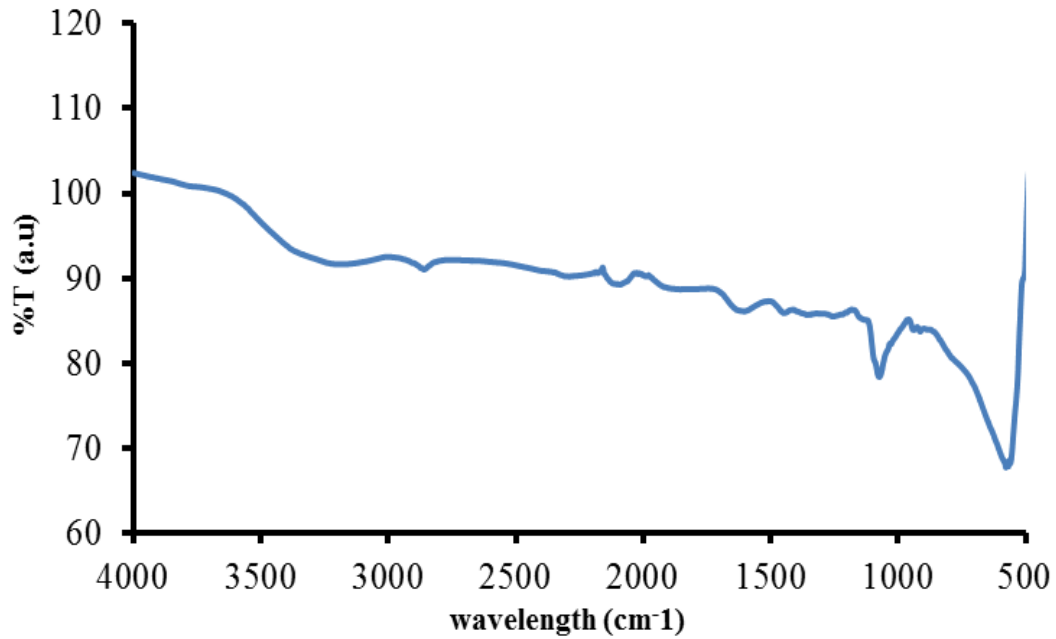


Figure 3.7: FTIR spectra of G-TiO₂ nanocomposites.

From the figure 3.7, it has been observed that there are peaks at 577 cm⁻¹, 1074 cm⁻¹, 1485 cm⁻¹, 1603 cm⁻¹, 2094 cm⁻¹, 2288 cm⁻¹, 2860 cm⁻¹, 3232 cm⁻¹. The strong absorption band around 577 cm⁻¹ indicates the vibration band of Ti-O-Ti bonds in TiO₂. The absorption band around 1603 cm⁻¹ can be attributed to the skeletal vibration of graphene sheet. [30].

3.5.5 UV-Visible Spectroscopy

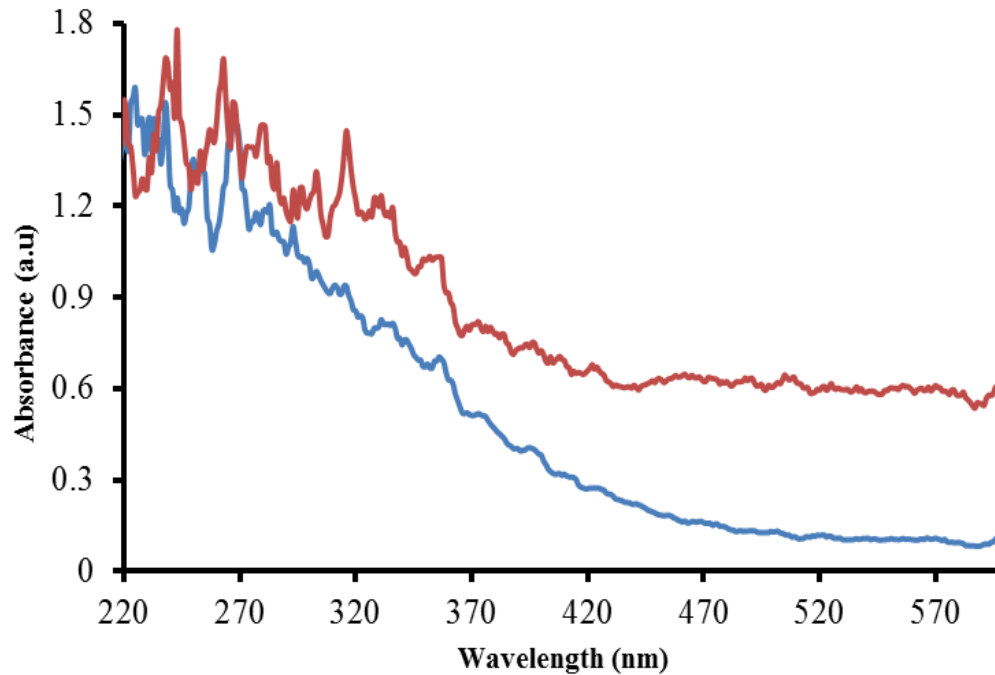


Figure 3.8: UV-visible absorption spectra of TiO₂ (p25) ,G-TiO₂ nanocomposites.

Figure 3.8 shows UV- visible reflectance spectra of commercially available TiO₂ (P25) and G-TiO₂. The shift for the G-TiO₂ nanocomposite towards the visible range and enhanced absorption indicates the presence of graphene. This is may be an indication that this material can work well like TiO₂ for photocatalysis but under visible range.

3.5.6 X-Ray Diffraction

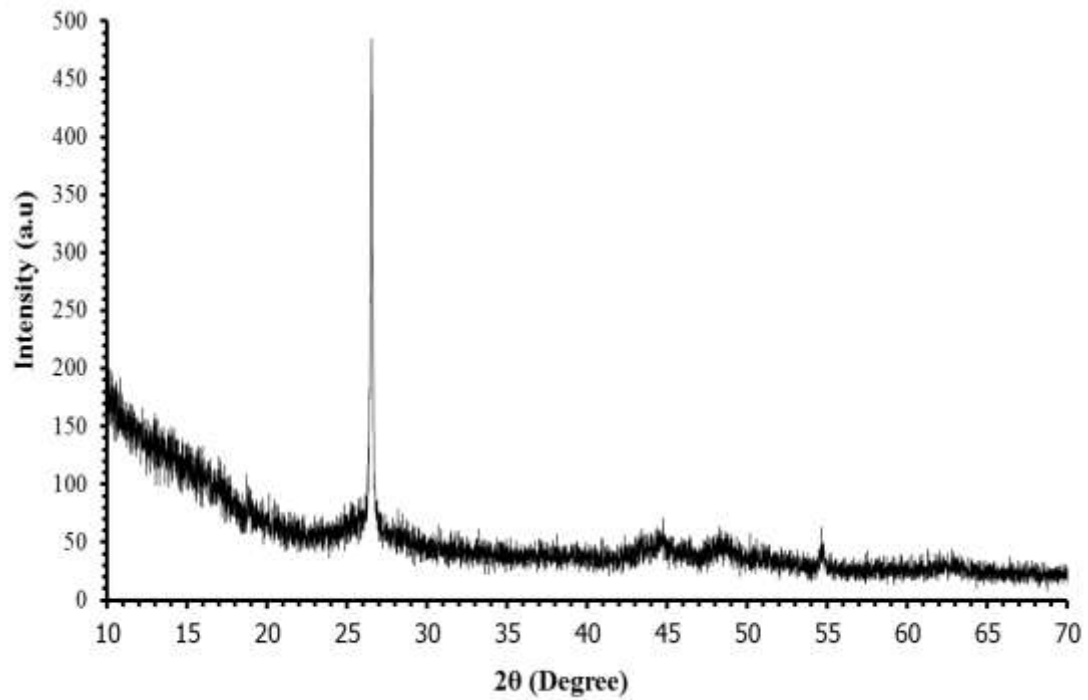
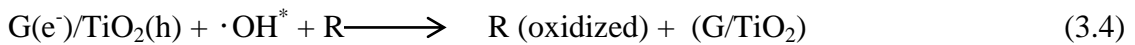
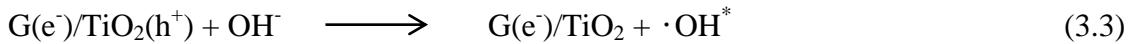
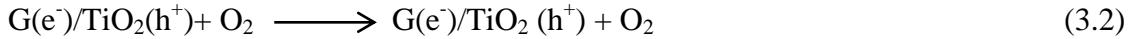


Figure 3.9: X-Ray diffraction pattern of G-TiO₂

From figure 3.9 X-Ray Diffraction peaks are seen at 26.505, 44.35, 48.036, 54.605, and 61.9 degree. Diffraction peaks exhibits at 26.505° and 48.03° indicating TiO₂ in the anatase phase of TiO₂ [34].

3.6 Organic Material Remediation Using G-TiO₂ Nanocomposite

When UV irradiation equal or more than the band gap falls upon the TiO₂, electrons from valance band get excited and move to the conduction band, hence form electron and hole pairs. These holes oxidize the H₂O and generate OH* radicals and the electron is responsible for the reduction process on the TiO₂ surface [5]. However, recombination time of electrons and holes in TiO₂ is much more rapid than the time of chemical interaction of TiO₂ with the adsorbed contaminants, which diminishes the efficiency of the photocatalytic activity [6-8]. Graphene sheets can be used as a good support for TiO₂ to increase the photocatalytic activity as it has high specific surface area and unique electronic properties, and due to acceptance of electron by graphene giving rise to production of more OH* radicals [31]. The mechanism is shown in figure 3.10.



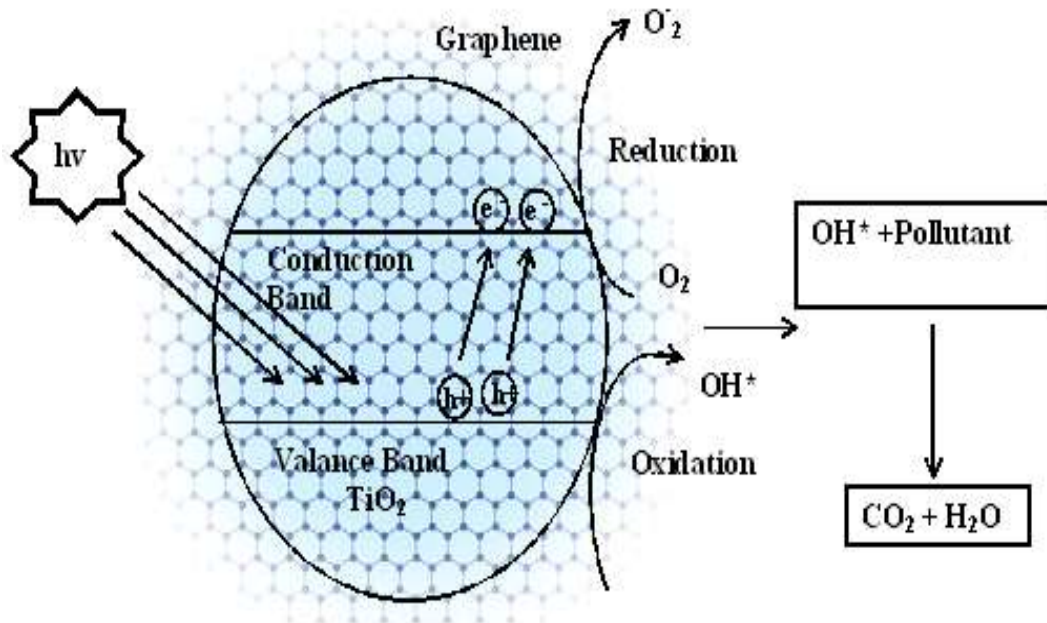


Figure 3.10: Mechanism of the photocatalytic effect of G-TiO₂. Adapted from [31].

3.6.1 Photocatalytic Measurement

In this process, 0.2 g of photocatalysts (G-TiO₂, G-SiO₂ and commercially available P25) was coated on the petri dish with the aid of asceic acid and kept at room temperature for drying under natural convection. This photocatalysts then heated at 200° C for 30 minutes before using it for photocatalytic degradation. Photocatalytic activities of this photocatalysts were appraised by photo degradation of methyl orange (MO). For this process, 40 ml MO of 20 ppm was taken into the each coated petri dishes and this setup was irradiated under UV-visible light. The illumination intensity was 30 W/ m². Similar setup was made and irradiated under normal 60 W bulbs. Distance between the bulb and petri dishes was 16 cm. After certain irradiation time interval, 1 ml of the MO was collected from the petri dishes and centrifuged to remove the photocatalyst. For each

sample, concentration of the upper clear layer was measured by recording the maximum absorbance of MO with the aid of Ocean Optics UV-visible spectrophotometer.



Figure 3.11: G-TiO₂ coated petri dish'



Figure 3.12 G-SiO₂ coated petri dish

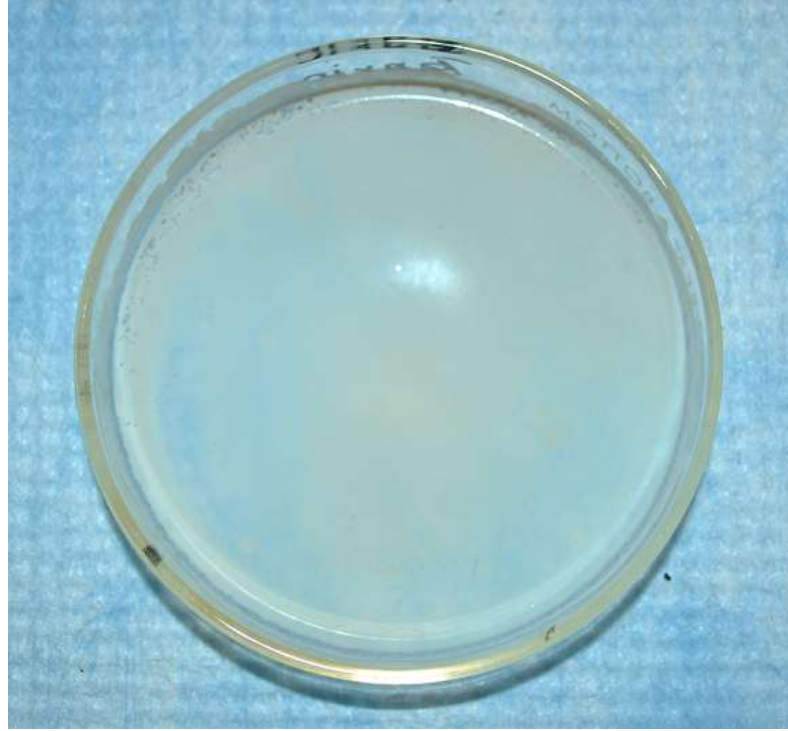


Figure 3.13: TiO₂ coated petri dish

3.6.2 Finding of the Work

Photo degradation experiments were carried out using MO as the model organic pollutant in the water with the aid of photocatalysts under the simulated sunlight. With the increasing reaction time, the absorbance peaks of the collected samples were decreasing. It is considered that absorption peak (A) is proportional to the concentration (C). So it can be assumed that change of the absorbance (A/A_0) indicates the change of the concentration (C/C_0) where, A_0 and C_0 were the initial absorbance and initial concentration respectively.

Table 3.1: Concentration change with irradiation time under UV-visible (30 W/ m²).

| Time | C/Co (p25) | C/Co (G-TiO2) | C/Co (G-SiO2) |
|------|------------|---------------|---------------|
| 195 | 0.02163294 | | 0.586368978 |
| 180 | 0.05373343 | 0.003340013 | 0.593419506 |
| 165 | 0.10467551 | 0.048096192 | 0.601057579 |
| 150 | 0.21004885 | 0.080828323 | 0.613983549 |
| 135 | 0.28820656 | 0.13760855 | 0.636310223 |
| 120 | 0.32240056 | 0.264529058 | 0.697414806 |
| 105 | 0.34891835 | 0.295925184 | 0.702115159 |
| 90 | 0.41591068 | 0.317301269 | 0.777320799 |
| 75 | 0.51290998 | 0.342017368 | 0.878378378 |
| 60 | 0.59525471 | 0.432197729 | 0.909518214 |
| 45 | 0.69644103 | 0.503006012 | 0.920094007 |
| 30 | 0.87578507 | 0.646626587 | 0.942420682 |
| 15 | 0.92254013 | 0.83500334 | 0.994124559 |
| 0 | 1 | 1 | 1 |

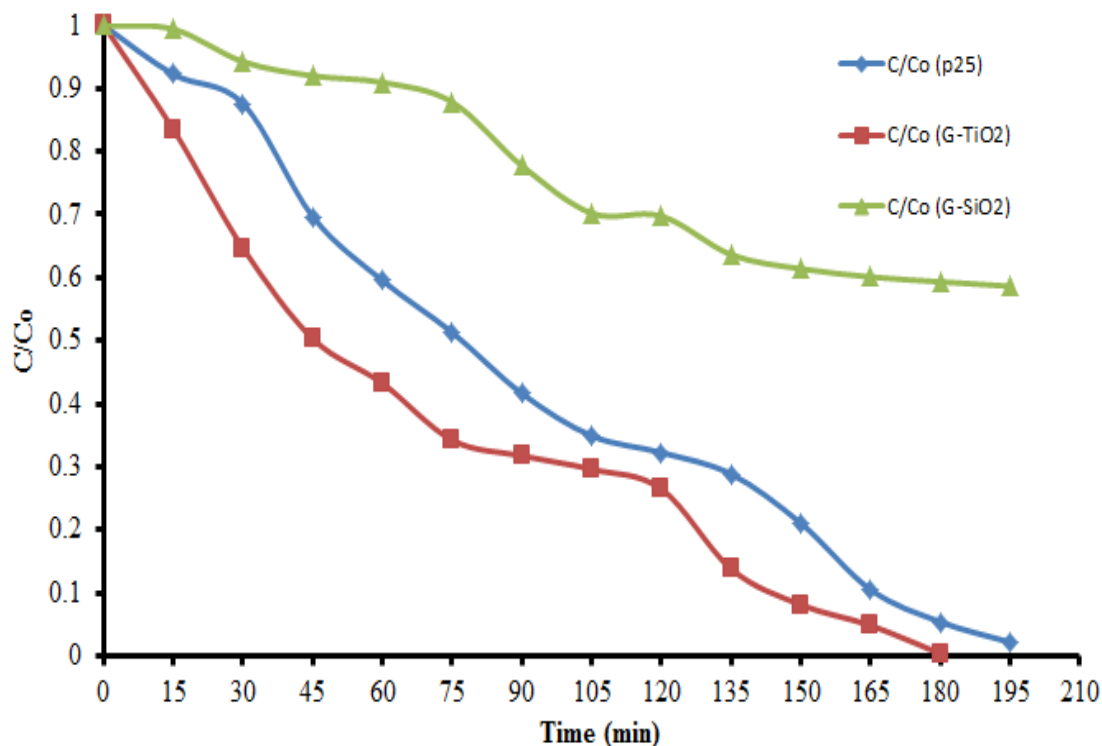


Figure 3.14: Photodegradation of MO by G-TiO₂, G-SiO₂ and commercially available P25 under irradiation of 30 W/m² UV-visible light.

In figure 3.14 it has observed that G-TiO₂ exhibits higher photocatalytic activity than commercially available p25 and G-SiO₂. For G-TiO₂, it took 180 minutes under the UV-visible light to degraded MO completely whereas it took almost 195 minutes for the commercially available P25 to clear the water. G-SiO₂ also showed promising activity in photo catalysis as it reduced the concentration to 60% of its original concentration.



Figure 3.15: Samples collected after certain irradiation time intervals for G-TiO₂

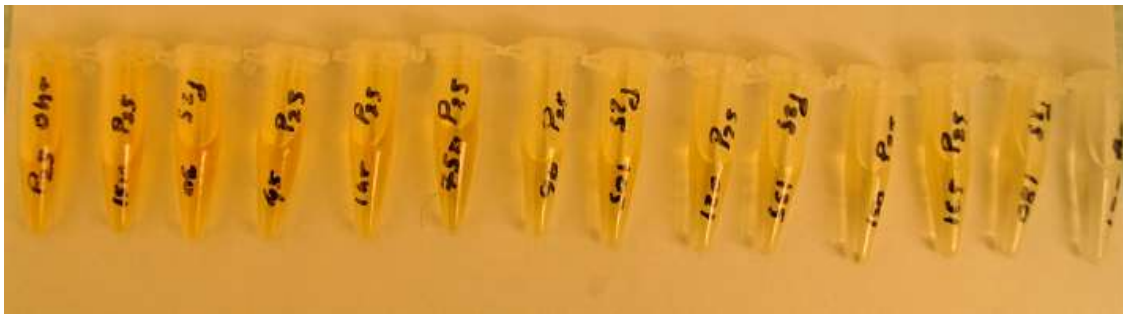


Figure 3.16: Samples collected after certain irradiation time intervals for P25

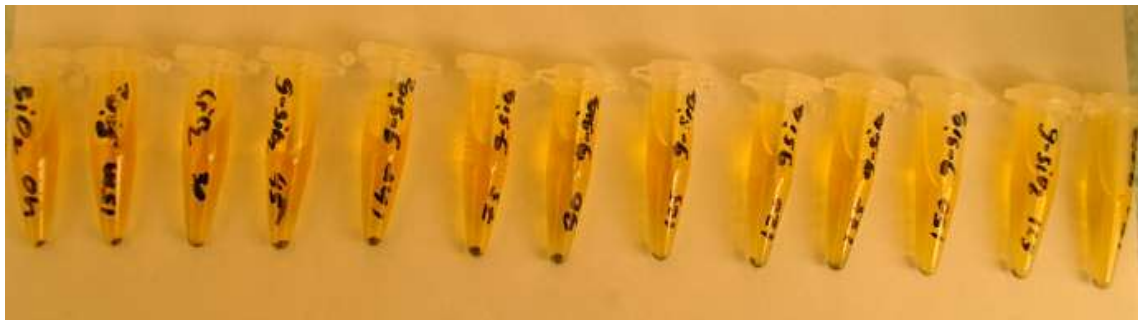


Figure 3.17: Samples collected after certain irradiation time intervals for P25

Similar setup was made and kept under normal 60 W bulbs. Distance between the bulb and petri dishes was 16 cm. In this case, it took longer irradiation time. Every 1 hour time interval, 1 ml of the MO was collected from the petri dishes and centrifuged to

remove the photocatalyst. For each sample, concentration of the upper clear layer was measured by recording the maximum absorbance of MO with the aid of Ocean Optics UV-visible spectrophotometer.

This measurement indicates that G-TiO₂ takes less time than P25 to decontaminate the MO from water. This observation was continued for 8 hours. Results indicated that kinematic rate of organic material removal for G-TiO₂ is higher than P25 under 60 W normal bulb.

Table 3.2 Concentration change with irradiation time under normal soft light

| Time | c/co (G-TiO ₂) | c/co (P25) |
|------|----------------------------|------------|
| 0 | 1 | 1 |
| 60 | 0.82412791 | 0.9310345 |
| 120 | 0.77616279 | 0.8784893 |
| 180 | 0.74854651 | 0.862069 |
| 240 | 0.70348837 | 0.8070608 |
| 300 | 0.59956395 | 0.729064 |
| 360 | 0.56686047 | 0.6075534 |
| 420 | 0.50872093 | 0.5500821 |
| 480 | 0.40697674 | 0.4860427 |

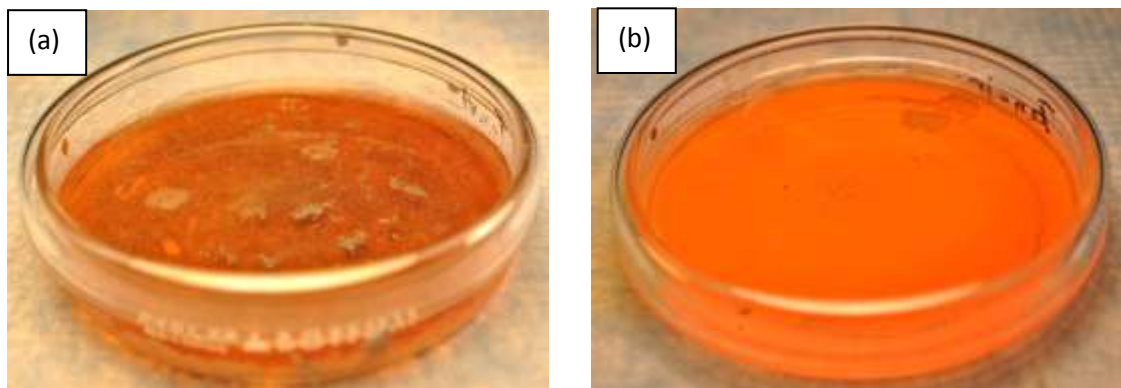


Figure 3.18: Coated petri dish with G-TiO₂ (a) and P25 (b) for photodegradation of MO under irradiation of 60 W normal



Figure 3.19: Setup for photodegradation of MO by G-TiO₂ under irradiation of 60 W normal bulb



Figure 3.20: Setup for photodegradation of MO by P25 under irradiation of 60 W normal bulb

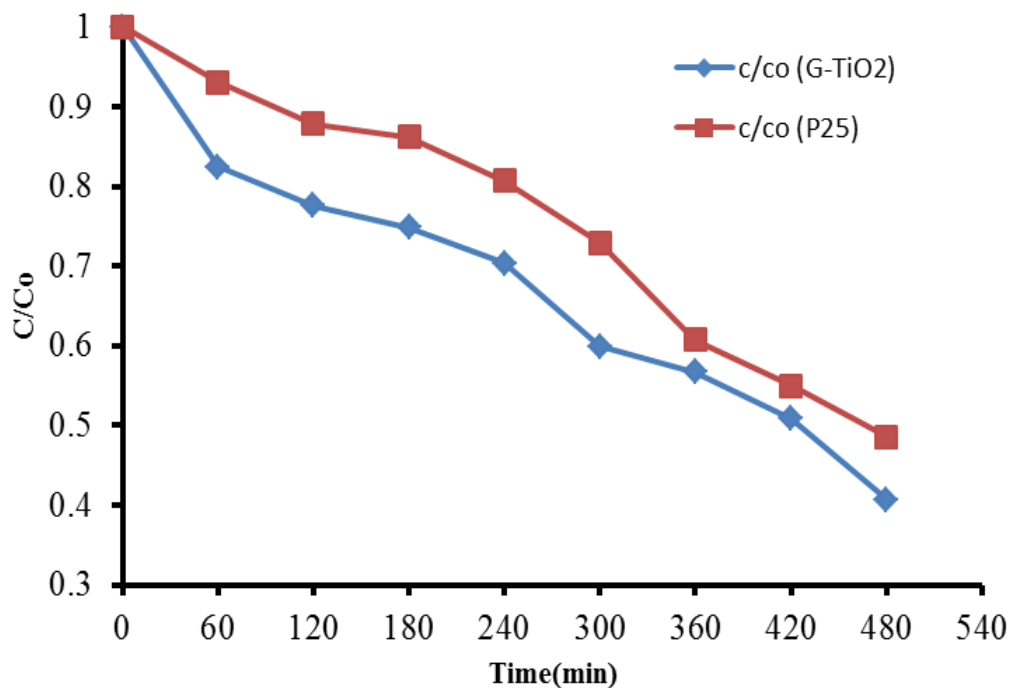


Figure 3.21: Photodegradation of MO by G-TiO₂ and commercially available P25 under irradiation of 60 W normal bulb

3.7 Summary

These results indicate that G-TiO₂ is better photocatalytic material than P25. It is removing the MO from the water quicker than commercially available P25. Graphene in the nanocomposite block the electron hole pair recombination as it acts as an electron accepting material. Thus good distribution of TiO₂ particles on graphene shows good photocatalytic activity [31]. This composite may find a significant application in the field of water decontamination.

3.8 References

- [1] A. Fujishima and K. Honda, *Nature*, 1972, 238, 37.
- [2] K. Rajeshwar, N. R. de Tacconi and C. R. Chenthamarakshan, *Chem. Mater.*, 2001, 13, 2765.
- [3] Y. Chen, J. C. Crittenden, S. Hackney, L. Sutter and D. W. Hand, *Environ. Sci. Technol.*, 2005, 39, 1201.
- [4] Y. Chen and D. D. Dionysiou, *Appl. Catal., A*, 2007, 317, 129.
- [5]. Manoj K. Ram and Ashok Kumar Decontamination Using Nanotechnology, Book Chapter 1
- [6] K. Woan, G. Pyrgiotakis and W. Sigmund, *Adv. Mater.*, 2009, 21, 2233.
- [7] M. R. Hoffmann, S. T. Martin, W. Y. Choi and D. W. Bahnemann, *Chem. Rev.*, 1995, 95, 69
- [8] D. Robert, *Catal. Today*, 2007, 122, 20–26
- [9] V. Subramanian, E. E. Wolf and P. V. Kamat, *Langmuir*, 2003, 19, 469.
- [10] K. H. Ji, D. M. Jang, Y. J. Cho, Y. Myung, H. S. Kim, Y. Kim and J. Park, *J. Phys. Chem. C*, 2009, 113, 19966.
- [11] D. Kannaiyan, E. Kim, N. Won, K. W. Kim, Y. H. Jang, M. A. Cha, D. Y. Ryu, S. Kim and D. H. Kim, *J. Mater. Chem.*, 2010, 20, 677.
- [12] S. Shanmugam, A. Gabashvili, D. S. Jacob, J. C. Yu and A. Gedanken, *Chem. Mater.*, 2006, 18, 2275.
- [13] L. Yang, S. Luo, S. Liu and Q. Cai, *J. Phys. Chem. C*, 2008, 112, 8939.
- [14] H. Yu, X. Quan, S. Chen and H. Zhao, *J. Phys. Chem. C*, 2007, 111, 12987.
- [15] Y. Yu, J. C. Yu, C. Y. Chan, Y. K. Che, J. C. Zhao, L. Ding, W. K. Ge and P. K. Wong, *Appl. Catal., B*, 2005, 61, 1.
- [16] Y. Yao, G. Li, S. Ciston, R. M. Lueptow and K. A. Gray, *Environ. Science Technology.*, 2008, 42, 4952.
- [17] X. H. Xia, Z. J. Jia, Y. Yu, Y. Liang, Z. Wang and L. L. Ma, *Carbon*, 2007, 45, 717.

- [18] W. Wang, P. Serp, P. Kalck and J. L. Faria, *Appl. Catal., B*, 2005, 56, 305.
- [19] E. Palacios-Lidon, B. Perez-Garcia, J. Abellan, C. Miguel, A. Urbina and J. Colchero, *Adv. Funct. Mater.*, 2006, 16, 1975.
- [20] Q. Liu, Z. Liu, X. Zhang, L. Yang, N. Zhang, G. Pan, S. Yin, Y. Chen and J. Wei, *Adv. Funct. Mater.*, 2009, 19, 894.
- [21] A. K. Geim and K. S. Novoselov, "The rise of graphene," *Nat Mater*, vol. 6, no. 3, pp. 183-191, Mar. 2007.
- [22] J. C. Meyer, A. K. Geim, M. I. Katsnelson, K. S. Novoselov, T. J. Booth, and S. Roth, "The structure of suspended graphene sheets," *Nature*, vol. 446, no. 7131, pp. 60-63, Mar. 2007.
- [23] H.-P. Huang and J.-J. Zhu, "Preparation of Novel Carbon-based Nanomaterial of Graphene and Its Applications Electrochemistry," *Chinese Journal of Analytical Chemistry*, vol. 39, no. 7, pp. 963-971, Jul. 2011.
- [24] A. H. C. Neto, F. Guinea, N. M. R. Peres, K. S. Novoselov, and A. K. Geim, "The electronic properties of graphene," arXiv:0709.1163, Sep. 2007.
- [25] A. A. Balandin, S. Ghosh, W. Z. Bao, I. Calizo, D. Teweldebrhan, F. Miao and C. N. Lau, *Nano Lett.*, 2008, 8, 902–907.
- [26] K. I. Bolotin, K. J. Sikes, Z. Jiang, M. Klima, G. Fudenberg, J. Hone, P. Kim and H. L. Stormer, *Solid State Commun.*, 2008, 146, 351–355.
- [27] B. Seger and P. V. Kamat, *J. Phys. Chem.C*, 2009, 113(19), 7990–7995.
- [28] D. Eder and A. H. Windle, *Adv. Mater.*, 2008, 20, 1787.
- [29] H. Cao, Y. Zhu, X. Tan, H. Kang, X. Yang and C. Li, *New J. Chem.*, 2010, 34, 1116.
- [30] C. Nethravathi and M. Rajamathi, *Carbon*, 2008, 46, 1994.
- [31] Kangfu Zhou, Yihua Zhu, Xiaoling Yang, Xin Jiang and Chunzhong Li Preparation of graphene–TiO₂ composites with enhanced photocatalytic activity, *Journal of Materials Chemistry* 7th January 2010
- [32] I Calizo, D Teweldebrhan W Bao, F Miao, C N Lau and A A Balandin Spectroscopic Raman Nanometrology of Graphene and Graphene

Multilayers on Arbitrary Substrates Journal of Physics: Conference Series
109 (2008) 012008

- [33] C. Stampfer, a F. Molitor, D. Graf, and K. Ensslin Raman imaging of doping domains in graphene on SiO₂, Applied Physics Letters 91, 241907 2007.
- [34] Kheamrutai Thamaphat, Pichet Limsuwan and Boonlaer Ngotawornchai, Phase Characterization of TiO₂ Powder by XRD and TEM, Kasetsart J. (Nat. Sci.) 42 : 357 - 361 (2008).

Chapter 4

Synthesis, Characterization of G-SiO₂ and Application in Heavy Metal Removal

4.1 Introduction

Graphene, two dimensional allotrope of carbon [1] has exciting structural [2], electrochemical [3], physicochemical and electronic properties [4], and finds its applications in supercapacitors [5], sensor, biosensor [6], transparent conductor and photovoltaic devices [7-8]. The chemistry of the interface of graphene (G) with metal oxide has largely remained unexplored because researchers have mostly studied the pristine graphene structure [9-11]. The graphene fabricated on silicon dioxide (SiO₂) depicts the interesting electronic properties due to the local atomic configuration, and the binding sites of graphene with SiO₂. It has been reported that SiO₂ shows qualitative surface defect type dependency between the interactions of graphene with SiO₂ calculated from the first principle calculation [12].

Under this work, G-SiO₂ nanocomposite is synthesized using different molar ratios of precursor of SiO₂ and graphene by the hydrolysis using commercial graphene platelets. The G-SiO₂ nanocomposite was characterized by using Raman spectroscopy, FTIR, cyclic voltammetry, impedance, Scanning Electron Microscopy (SEM), Transmission Electron Microscopy (TEM) techniques, respectively. After that this nanoparticle is used for adsorption process in ZnCl₂ Solution.

4.2 Materials for G-SiO₂

The tetraethyl orthosilicate (TEOS), hydrochloric acid (HCl), propanol and acetone are all A.C.S. grade, and purchased from Sigma–Aldrich (USA). The graphene platelets (less than 20 nm in thickness) were purchased from Angstrom Materials (USA). All the chemicals and materials were employed as purchased without any modifications unless and until discussed in the manuscript.

4.3 Synthesis of G-SiO₂ Nanocomposite

The G-SiO₂ nanocomposite is synthesized using hydrolysis of tetraethylorthosilicate (TEOS) in presence of graphene nanoplatelets in a solution mixture containing propanol and diluted HCl solution. The TEOS (6.23gm) was mixed in a mixture solution containing propanol (15 mL), 0.03M of HCl (0.5 mL) and deionized water (15 mL). After that graphene (20 nm size) nanoplatelets were introduced in the mixture. The reaction was stirred at 300 rpm for 24 hours at room temperature. The resulting mixture was heated to a temperature of 80° C for 30 minutes under constant stirring forming white precipitate of SiO₂. The solution was centrifuged to remove the G-SiO₂ nanoparticles and later continuous cleaning was made to remove any organic residue using deionised water. The G-SiO₂ was dried for 4 hours at 100° C for the removal of water as well as any organic solvents. The table 1 also shows the ratio of different graphene to TEOS kept for synthesis of G-SiO₂ nanocomposite

Table 4.1: The parameters for the G-SiO₂ synthesis

| Sample | Propanol (ml) | HCl 0.03M (ml) | DI water (ml) | TEOS (gm) | Graphene (gm) | Time (min) | Temperature (°C) |
|--------|------------------|----------------------|---------------------|--------------|------------------|---------------|---------------------|
| S1 | 15 | 0.5 | 15 | 6.23 | 0.3 | 25-30 | 70-80 |
| S2 | 15 | 0.5 | 15 | 6.23 | 0.6 | 25-30 | 70-80 |
| S3 | 15 | 0.5 | 15 | 6.23 | 1.2 | 25-30 | 70-80 |

4.4 Flow Diagram of the Process

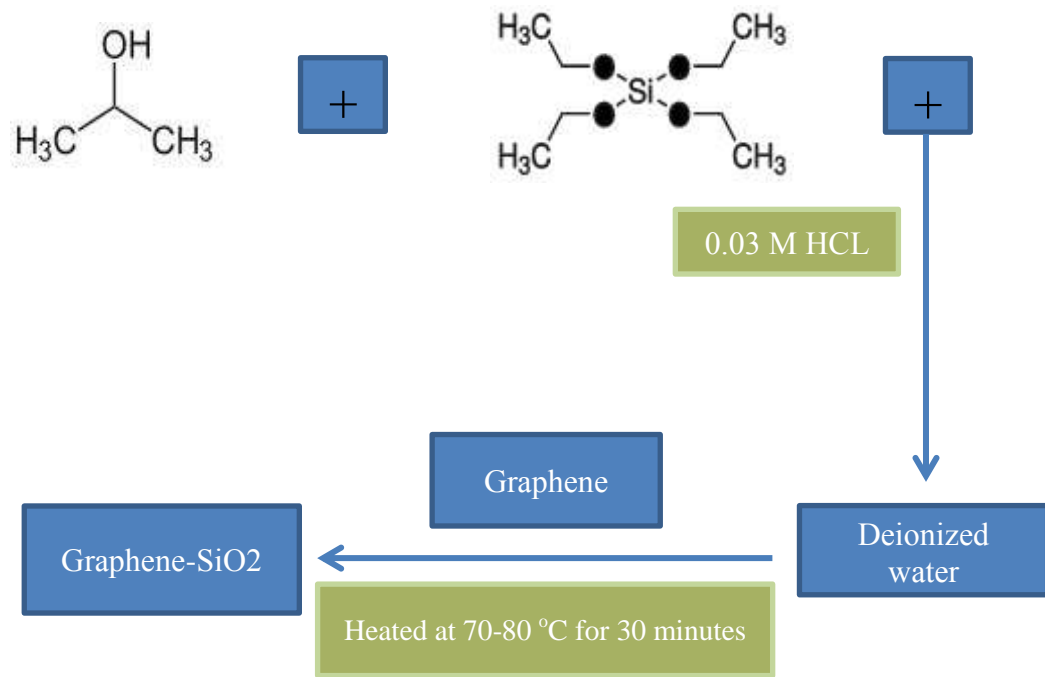


Figure 4.1 Flow diagram of G-SiO₂ synthesis process.

4.5 Characterization of G-SiO₂

4.5.1 Machine Specification and Sample Preparation

For several techniques (Raman, FTIR, XRD, SEM, TEM,) to characterize the G-SiO₂ nanocomposite, sample preparation methods were different. Raman spectra of G-SiO₂ nanocomposite were measured using a Renishaw Raman Spectroscopy through a 514nm laser beam. Raman samples were prepared by adding a small amount of dry powder to ethanol and then the solutions were coated on silicon substrates by spin coating. FTIR spectra of nanocomposite was performed under transmission mode using KBr pellet under Perkin Elmer spectrometer XRD analysis of G-SiO₂ samples were performed using X' Pert Pro system with Cu K α radiation ($\lambda = 1.54060\text{\AA}$) operated at 40 kV and 40 mA . For X-ray powder diffraction, samples were grinded well and put into the power holder. The SEM and TEM measurements were done to investigate the morphology of the surface of the nanocomposite by using Hithachi S-800 and Technai F20 respectively. The TEM samples were prepared by adding a small amount of dry powder to ethanol, and a small drop of a solution was dropped on 300 mesh copper TEM grids for the measurement. The electrochemical measurements on G-SiO₂ nanocomposite was investigated from cyclic voltammetry (CV), impedance and chronoamperometry measurements using VolatLab instrument. Samples were coated on ITO glasses. The CVs were recorded at different scan rates (100, 50, 25, 10 and 5 mV/s) to understand the G-SiO₂ electrochemical redox processes. The conductivity was measured through two probe measurement technique using Keithley Electrometer.

4.5.2 Raman Spectroscopy

Figure 4.2 shows the Raman spectra of samples S1, S2, and S3. The S1 shows the

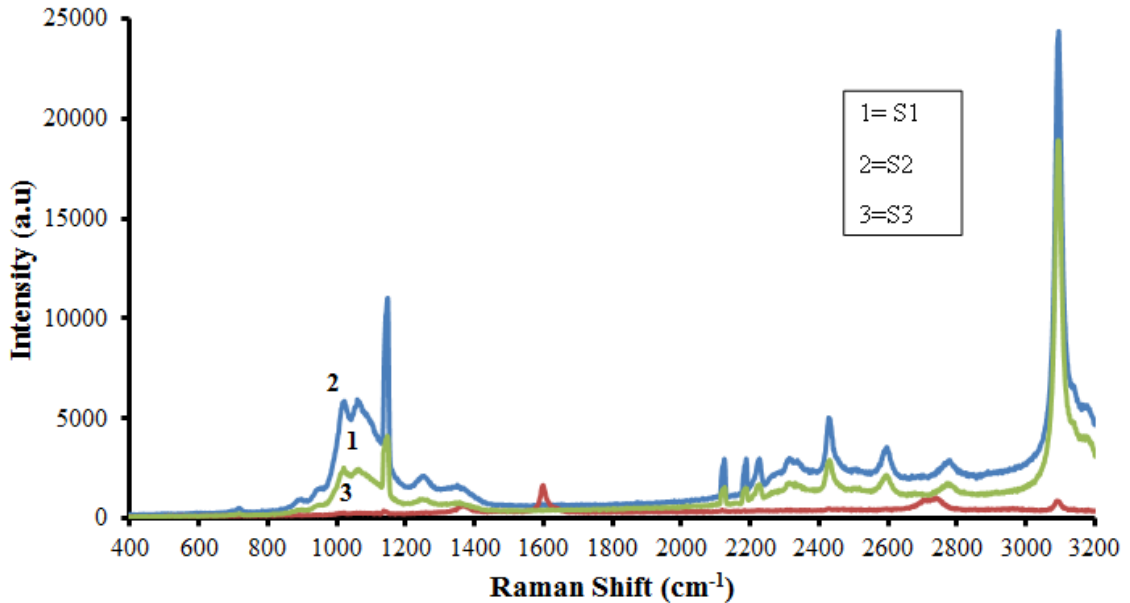


Figure 4.2: Raman spectra of G-SiO₂ for samples (S1, S2, S3 indicates different ratio of graphene and G-SiO₂).

Sample 1 Raman peak at 3100, 2788, 2606, 2418, 2327, 2209, 2198, 2130, 1617, 1372, 1267, 1153, 1177, 1031, 960 cm⁻¹. Sample 2 shows the Raman peaks at 3095, 2792, 2602, 2434, 2327, 2230, 2190, 2126, 1617, 1372, 1264, 1148, 1171, 1028, 960, 907, 730 cm⁻¹. The sample S3 shows the Raman peak at 3101, 2751, 2602, 2436, 1617, 1395, 1155 cm⁻¹. The graphene shows the D-peak around 1372 cm⁻¹ in G-SiO₂ sample which is generally observed at 1350 cm⁻¹ [13-14]. The Raman intensity of graphene shows the D-band at around 1372 cm⁻¹, G-peak around 1617 cm⁻¹, and the 2D-peak shifted 2788 cm⁻¹ from 2700 cm⁻¹

4.5.3 Fourier Transform Infrared (FTIR) Spectroscopy

Figure 4.3 shows the FTIR spectra of S1 (curve 1), S2 (curve 2) and S3 (curve 3) and SiO₂ (curve 4). This FTIR peaks have been observed similar to Raman spectrum.

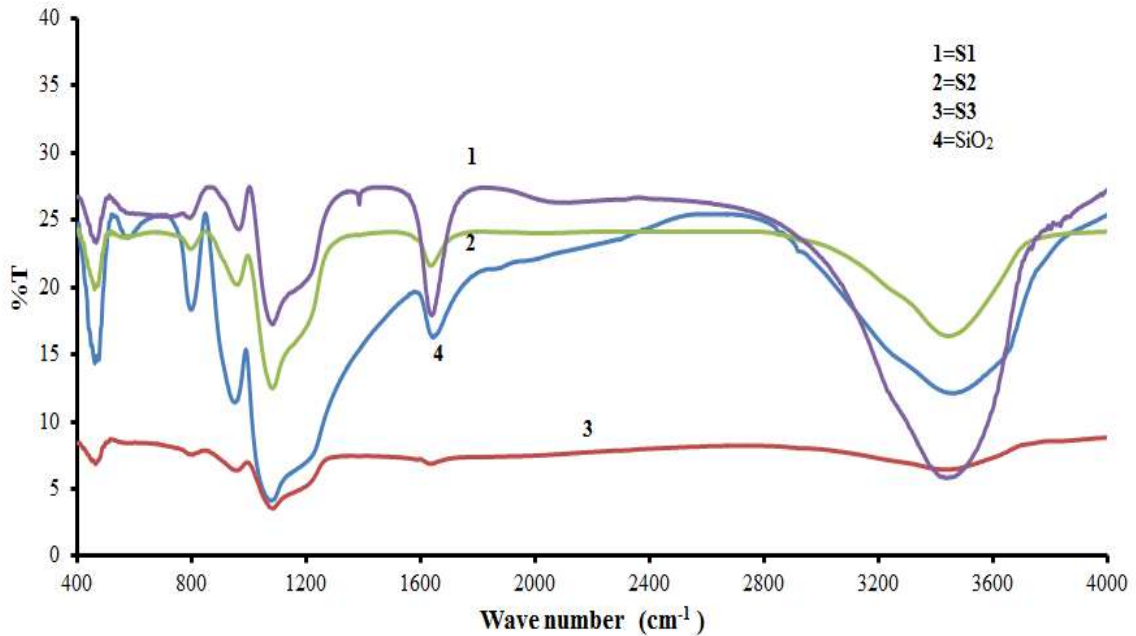


Figure 4.3: FTIR spectra of S1, S2, S3 (G-SiO₂ nanoparticles) and SiO₂ nanoparticles

The intensity of FTIR peak decreases as amount of graphene increases in G-SiO₂ nanocomposite. The peak at 1650 cm⁻¹ decrease with the increase of graphene contain in the sample whereas the peak at 1100 cm⁻¹ becomes sharper as the graphene percentage increases in G-SiO₂. Besides the sharp peaks observed at 958 cm⁻¹ and 800 cm⁻¹ in curve 4 reveal the presence of SiO₂. The peaks at 595 cm⁻¹ and 475 cm⁻¹ have also been found to decrease with the concentration of graphene from S1 to S3 samples.

4.5.4 Scanning Electron Microscopy (SEM)

Figure 4.4, 4.5 and 4.6 show the SEM images of samples S1, S2, S3 (table 4.1 show the composition of nanocomposite sample). The picture Figure 4.4 shows mostly the planner flakes structure.

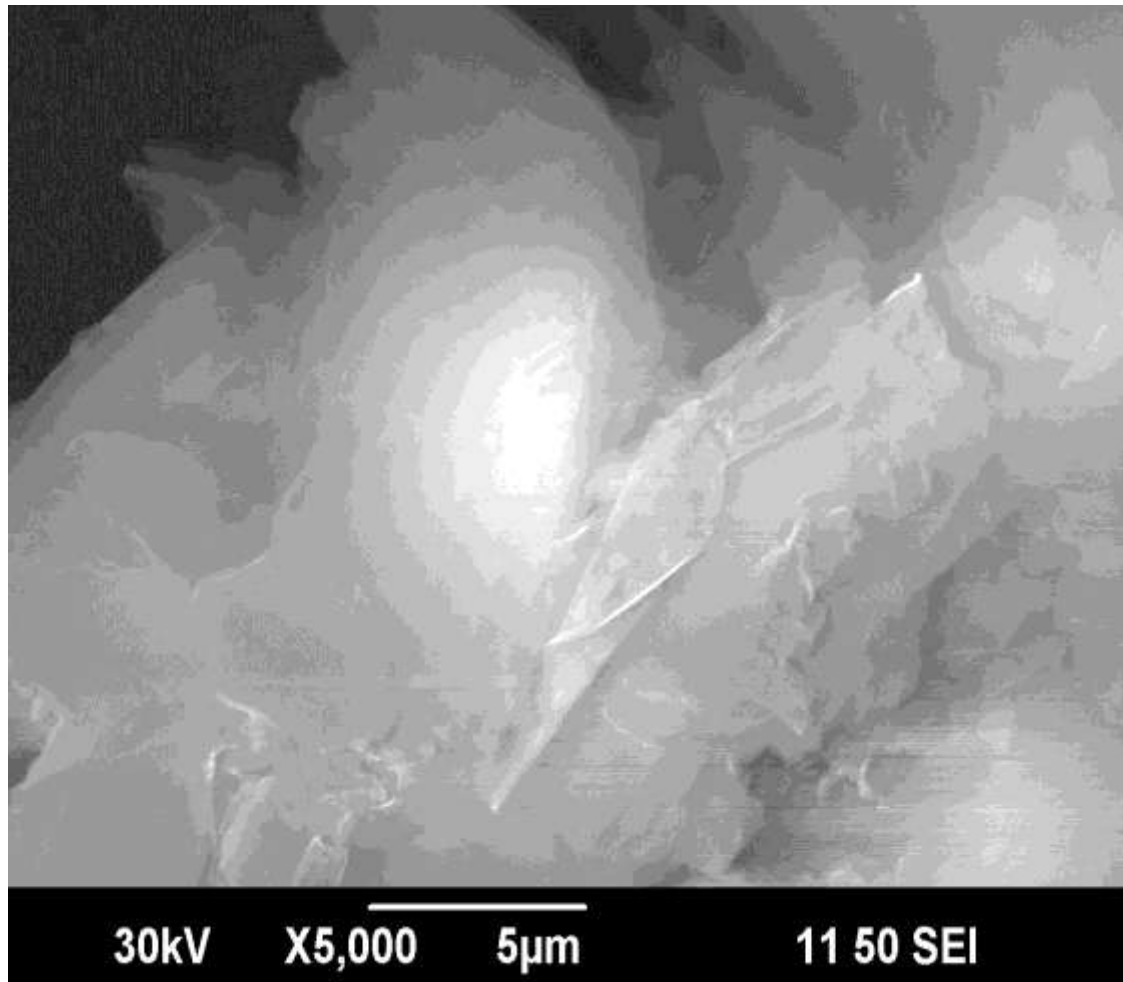


Figure 4.4: SEM image of G-SiO₂ (which indicates S1 composition)

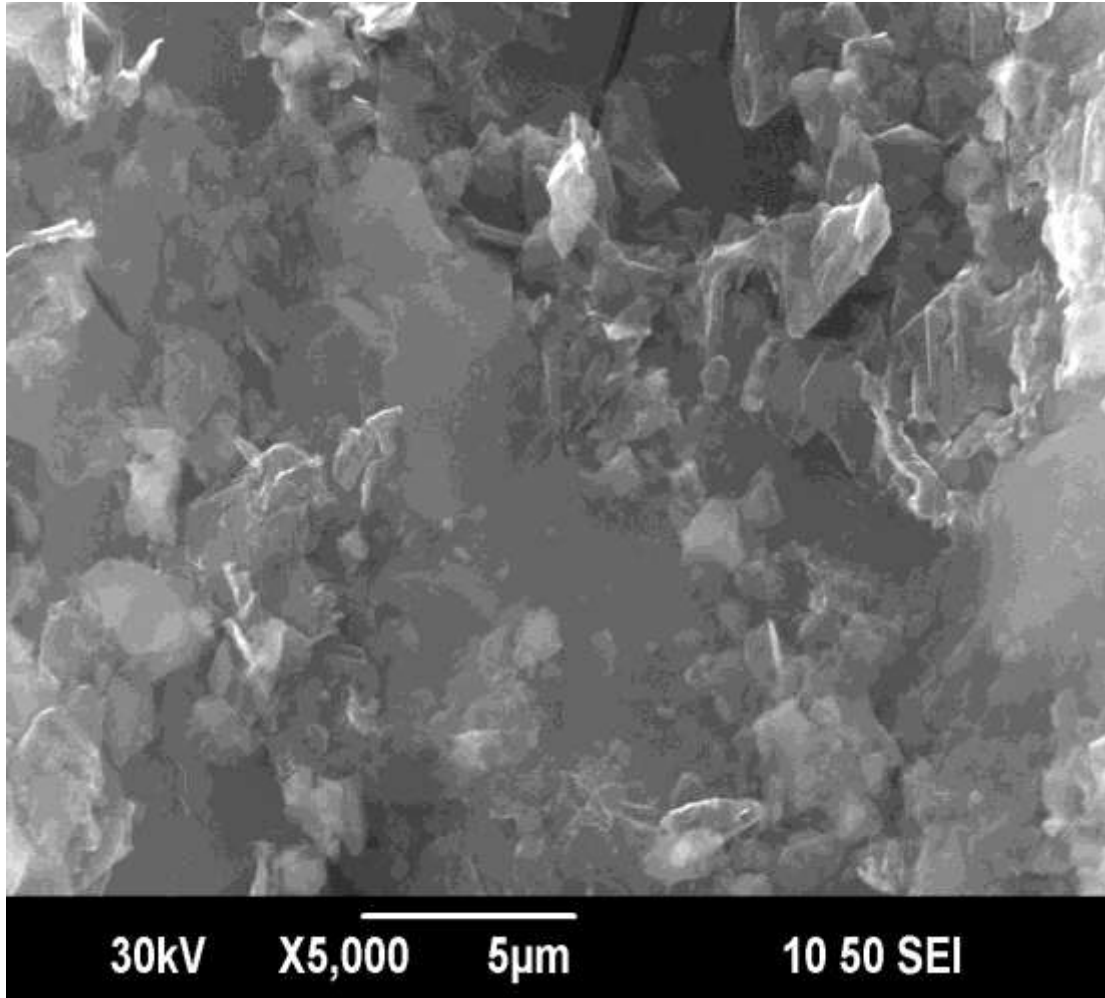


Figure 4.5: SEM image of G-SiO₂ (which indicates S2 composition)

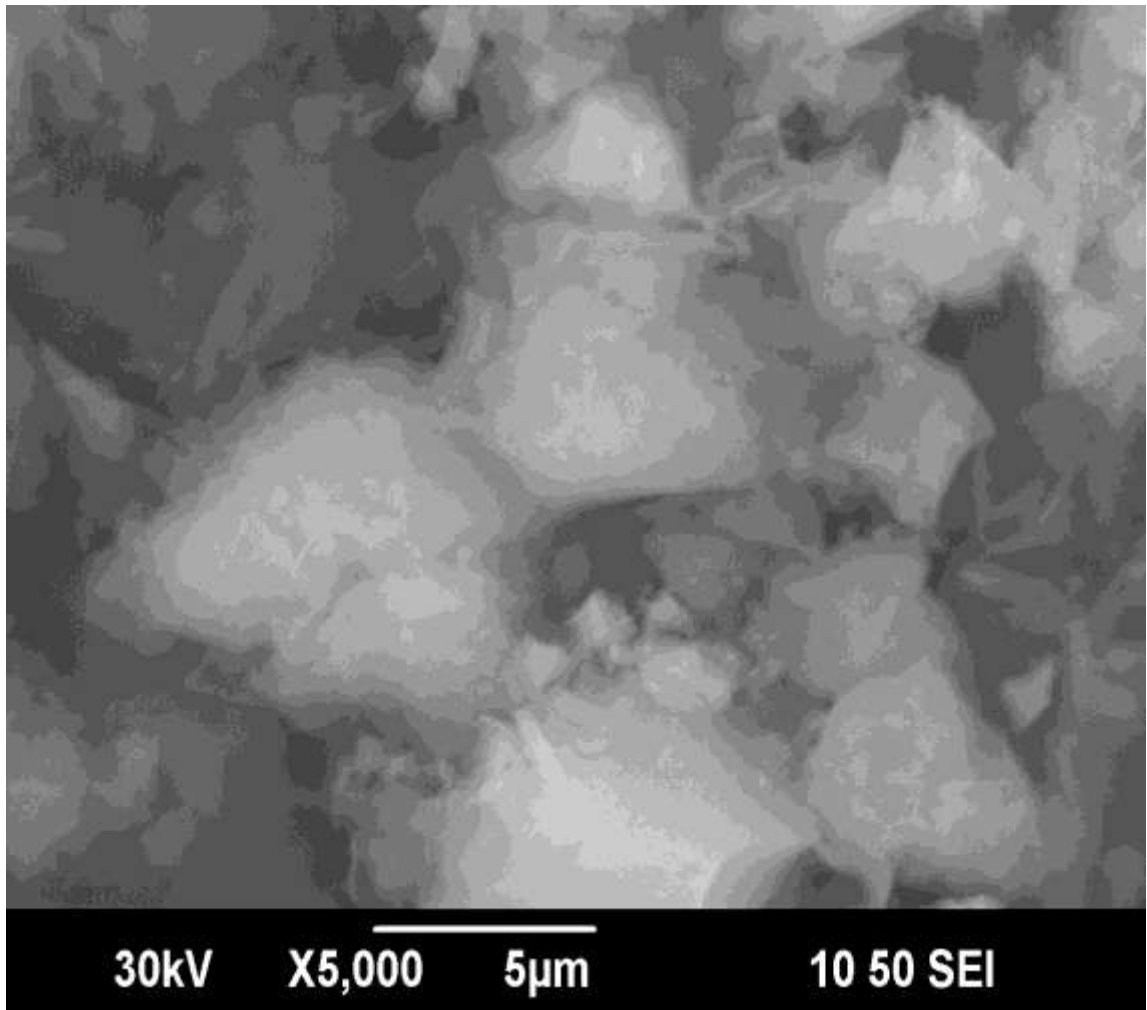


Figure 4.6: SEM image of G-SiO₂ (which indicates S3 composition)

The increase of graphene shows grains type of structure in Figure 4.5 whereas the flakes and woolen type of structure has been observed for the larger quantity of graphene in figure 4.6 nanocomposite sample.

4.5.5 Transmission Electron Microscopy (TEM)

Figure 4.7 shows the TEM picture of G-SiO₂ nanocomposite for the sample composition of TEOS to be 90% to 10% graphene. It show interesting feature as how the SiO₂ gets bundled of 20 to 50 nm with graphene nanoplates. Further, the graphene flakes composite with SiO₂ could be observed in the Figure 3.4.3.

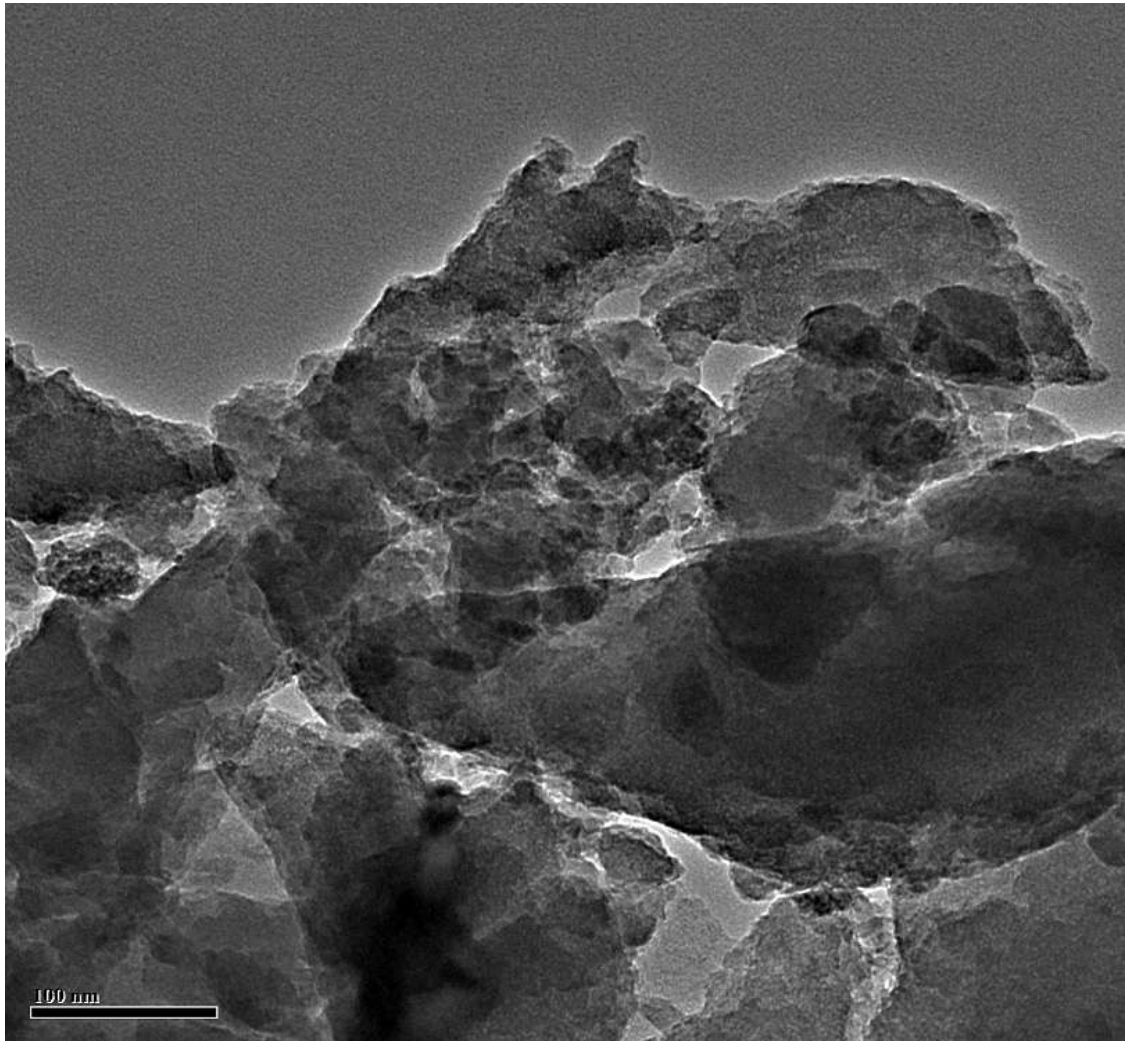


Figure 4.7: TEM image of G-SiO₂ (10% graphene -90% SiO₂) at 100 nm scale

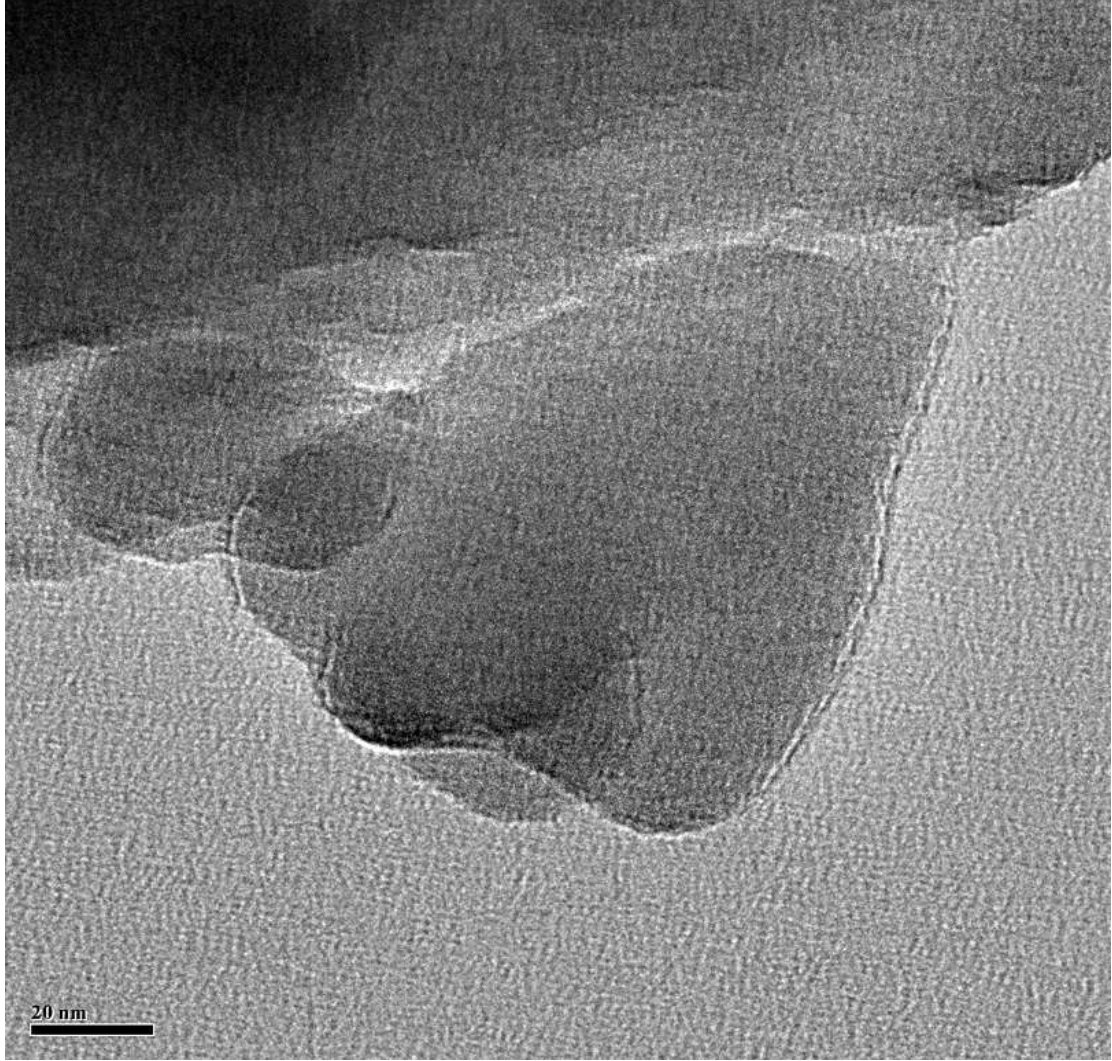


Figure 4.8: TEM image of G-SiO₂ (10% graphene -90% SiO₂) at 20 nm scale

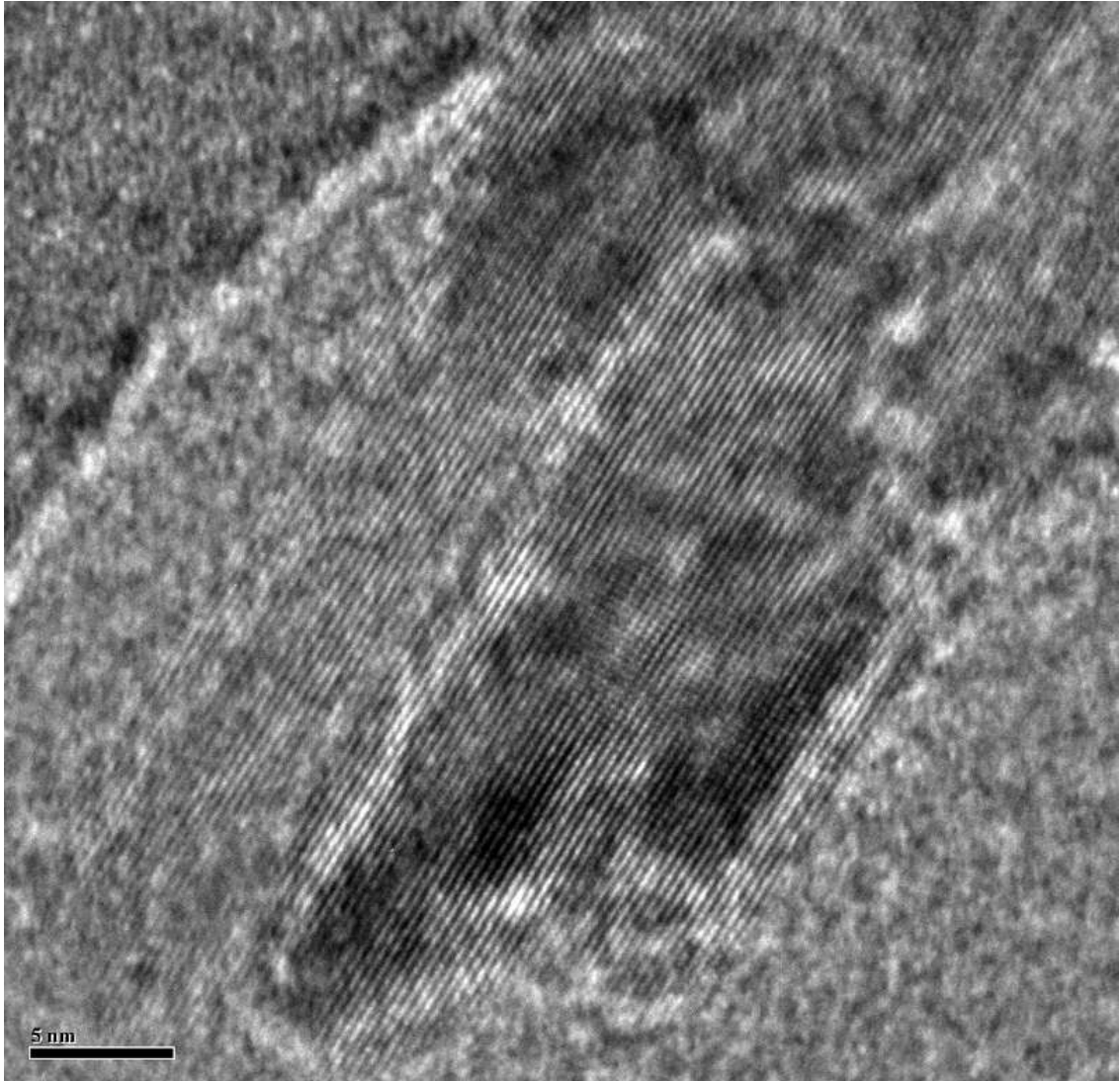


Figure 4.9: High resolution TEM image of G-SiO₂ (10% graphene -90% SiO₂)

4.5.6 X-Ray Diffraction

The S1 sample shows the diffraction peaks at 26.5, 46.3 and 54.7. The S2 sample shows the X-ray peak at 26.5, 42.4, 43.4, 44.6 and 46.3 and 54.67. The sample 3 shows the peak at 26.5, 42.5, 43.3, 44.4, 46.2 and 54.6. The diffraction peak is shown at $2\theta = 26.5^\circ$ with spacing as $d = 0.34$ nm. The literature shows that the peak with $d = 0.34$ nm corresponds to the normal graphite spacing [34]. The SiO_2 (curve 4) shows very wide peak from 22 to 28 degree indicating the amorphous nature of the nanomaterial

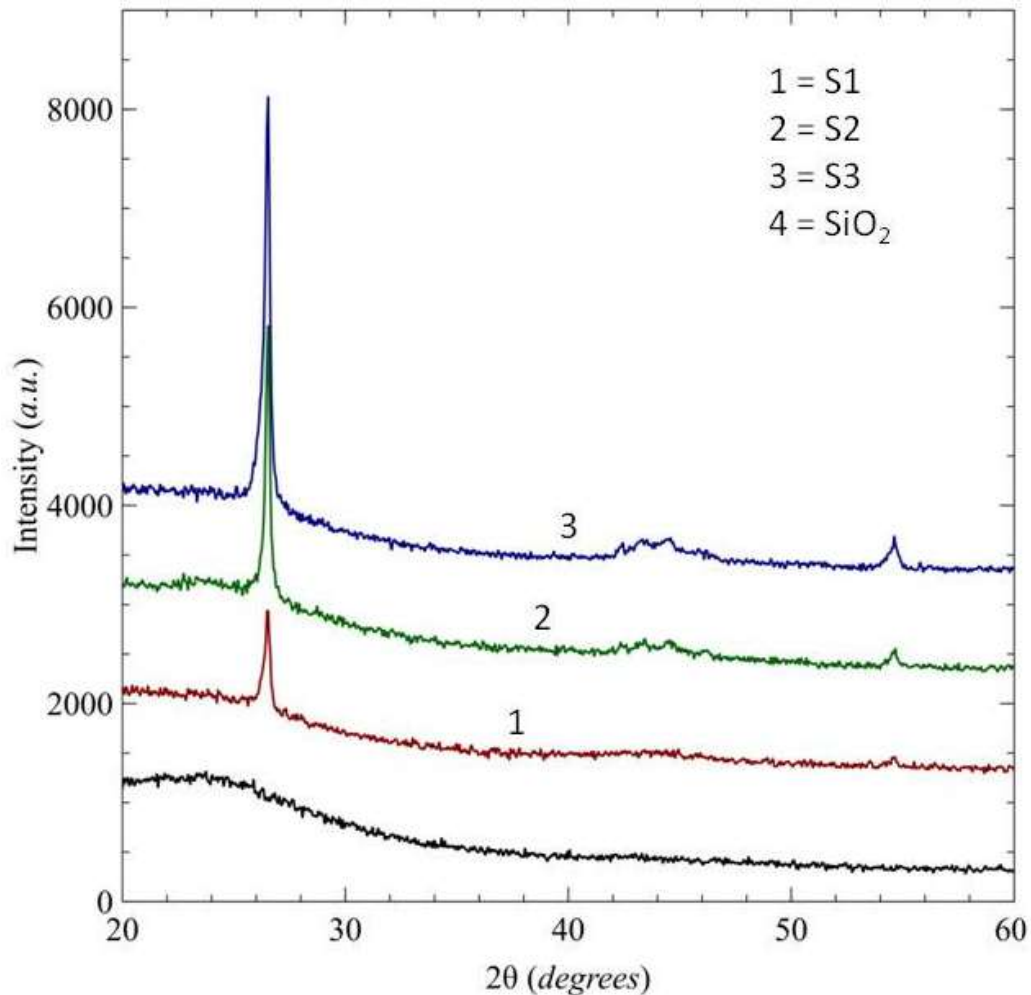


Figure 4.10: XRD of different amount of G- SiO_2

4.5.7 Cyclic Voltammetry

Figure 4.11 (S1, S2 and S3) shows the cyclic voltammetry curves as a function of scan rate. Figure 3S1 shows the CV of S1 with redox peak potentials at 1.69V and -0.29 V. Figure 3S2 shows the redox peaks at peak at 0.94 V and -0.39 V for S2, whereas the redox peaks are observed at 0.98V to -0.38V for sample S3 as shown in Figure 3S3. Figure 3S3 shows regular hysteresis with redox potential in CV curves, indicating a diffusional controlled system with the increase of graphene in G-SiO₂ nanocomposite.

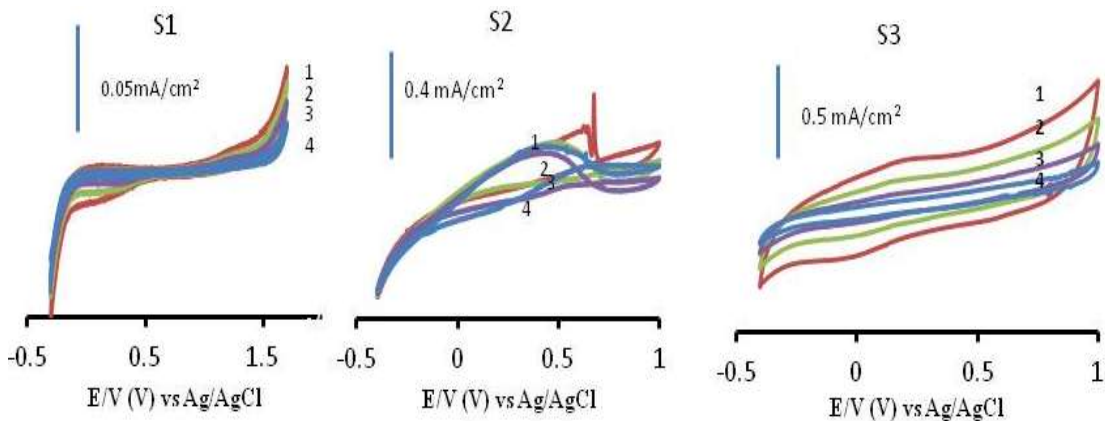


Figure 4.11 Cyclic voltammetry of G-SiO₂ (S1, S2 and S3) coated on ITO glass plate as working electrode, platinum as counter and Ag/AgCl as reference electrode in 0.1M TEATFF₄⁻ in acetonitrile solution

4.5.8 I-V Characteristics

Figure 4.12 shows the current (I) –voltage (V) characteristics of G-SiO₂ nanocomposite in two electrodes configuration. It has been found that at room temperature, with the increase of the amount of the graphene conductivity of the material increases.

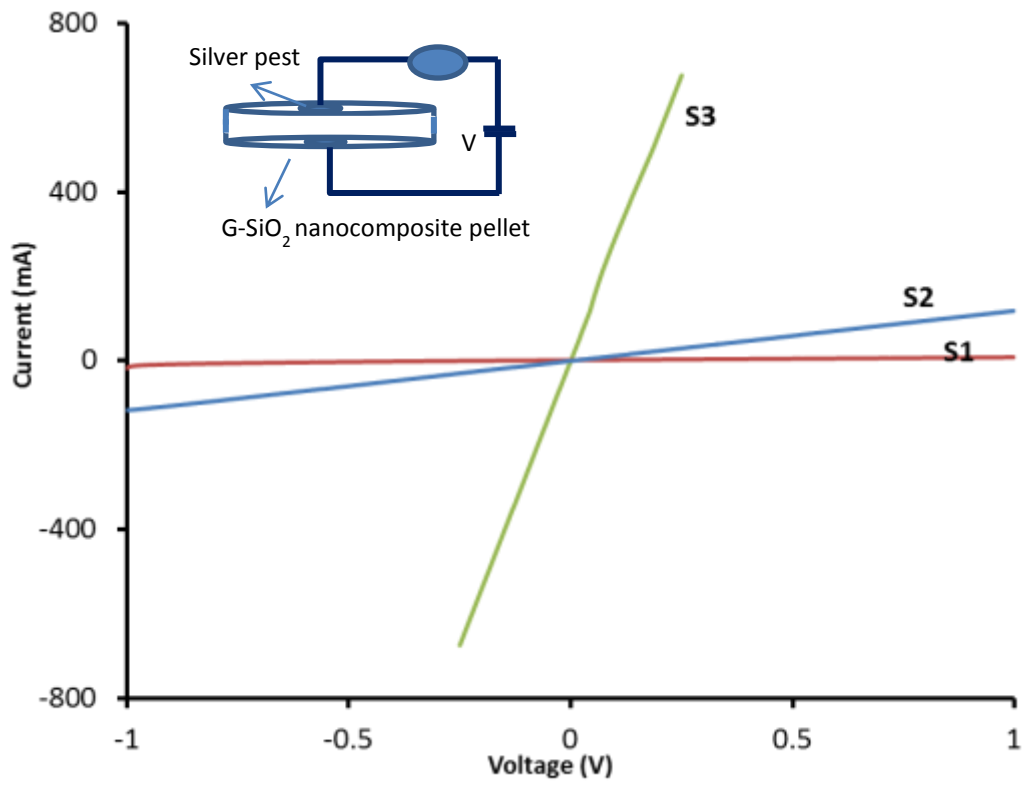


Figure 4.12: Current –Voltage characteristics of G-SiO₂ samples (S1, S2, S3) at room temperature.

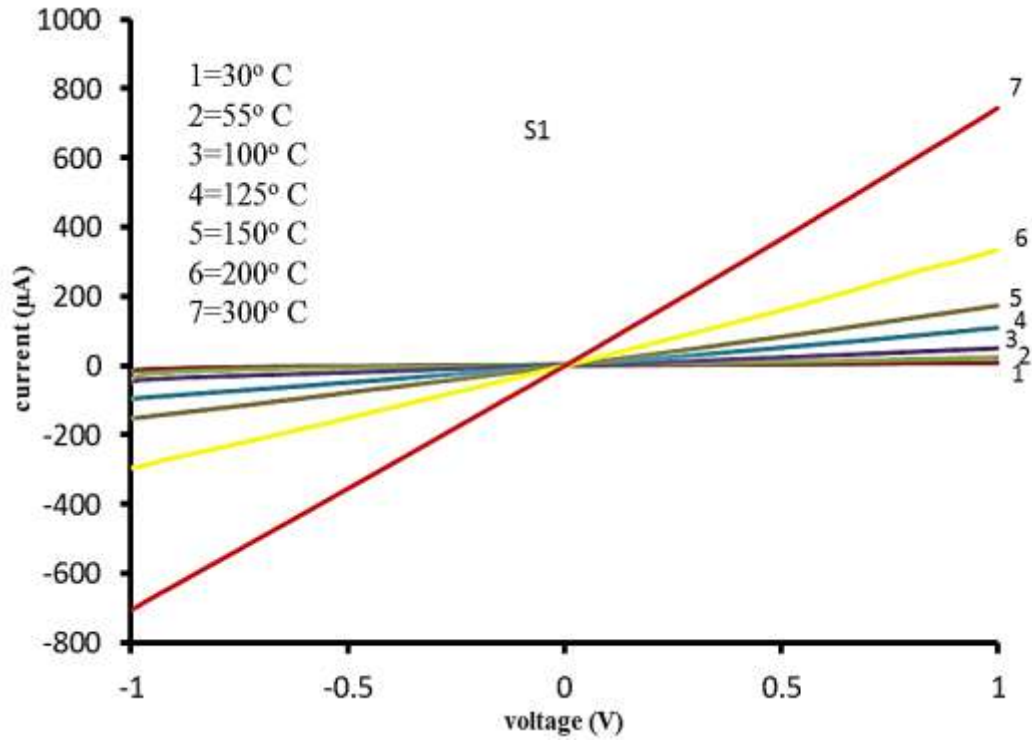


Figure 4.13: Current –Voltage characteristics of G-SiO₂ samples S1 at different temperature.

It has been observed in figure 4.13 that conductivity increases as the temperature increases which depict semiconducting properties of nanocomposite.

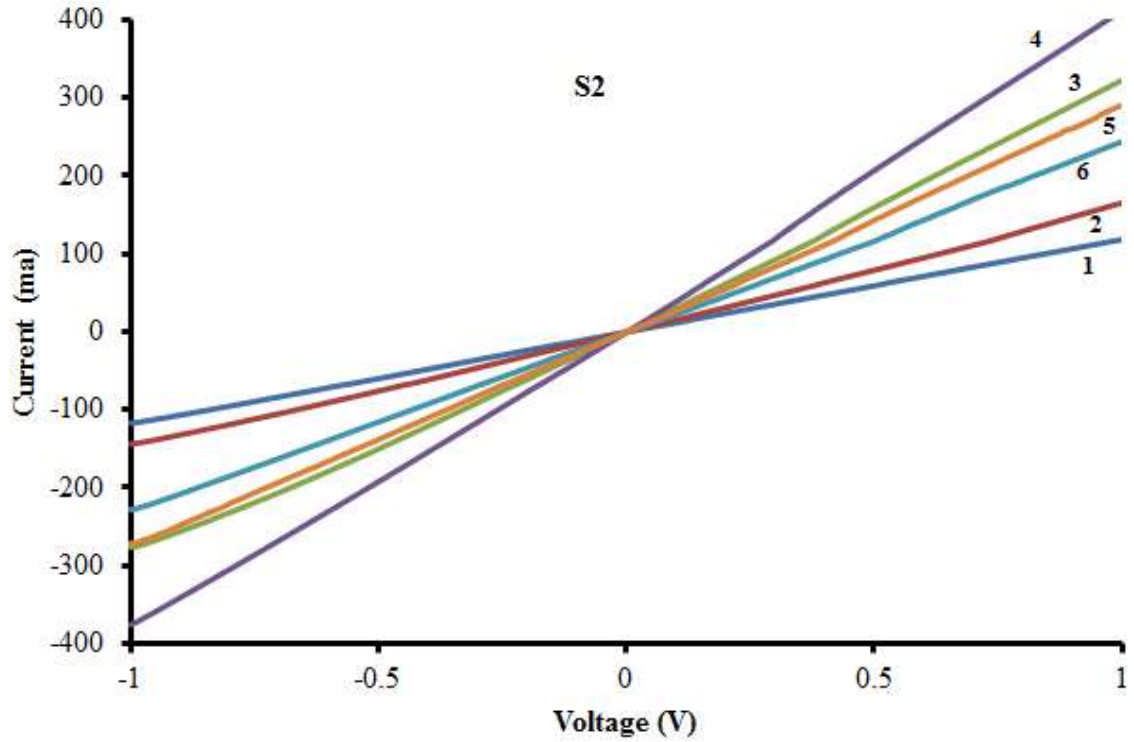


Figure 4.14: Current –Voltage characteristics of G-SiO₂ samples S2 at different temperature

The current has been found to be increasing till measured at 120° C indicating that G-SiO₂ below 120° C shows the metallic properties of nanocomposite where current decrease with the rise in temperature.

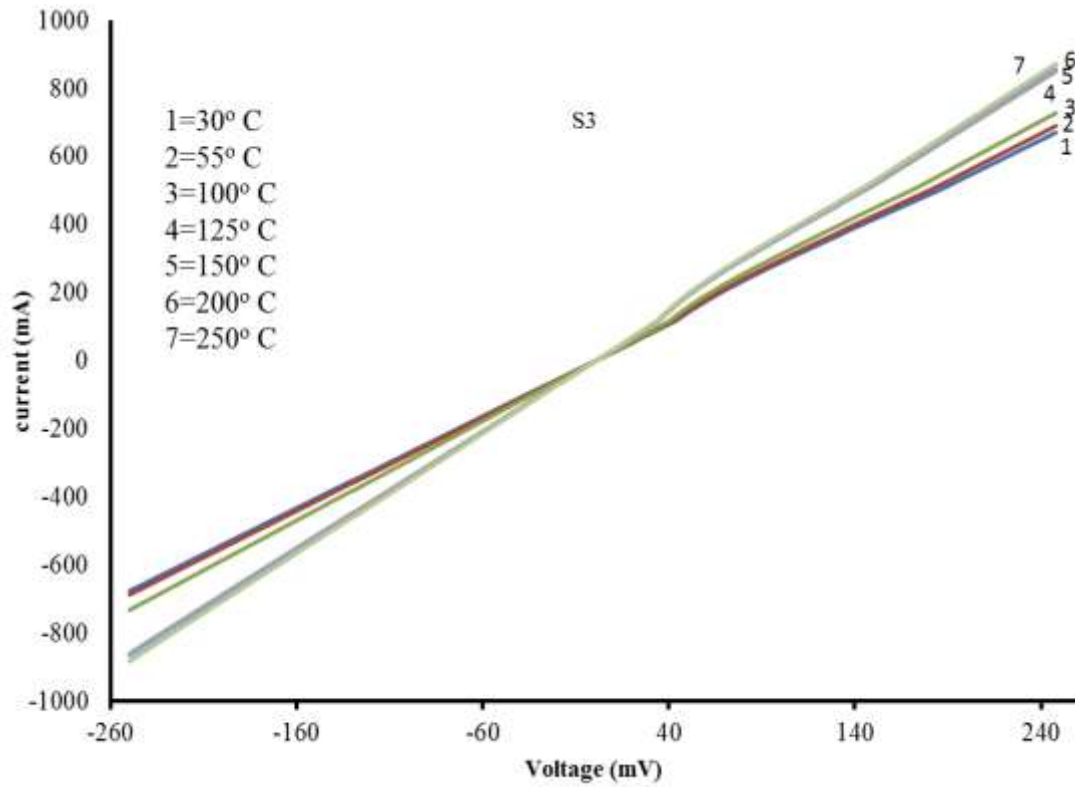


Figure 4.15: Current –Voltage characteristics of G-SiO₂ samples S3 at different temperature.

It has been observed in Figure 4.15 that conductivity increases as the temperature increases which indicates semiconducting properties of nanocomposite.

4.6 Heavy Metal Remediation from Water Using G-SiO₂

Presence of higher amount heavy metals in the ground water, drinking water and surface water has an intense impact on human survival. Wastewaters emits from industries contain large amount of heavy metals and to provide sustainable clean water we need to go through several techniques. In this thesis paper we put our main concern on Zn. There is a widespread realization that the presence of Zn ion in water is essential for some extent but when the quantity crosses the WHO standards then it is hazardous to human and ecosystem.

4.6.1 Adsorbate Solution and Adsorbent Preparation

In this experiment, two different stock solutions were prepared by dissolving 136.3 g of ZnCl₂ salt in deionized water. Stock solution was further diluted to get the desired molarity of the solution. Here, 0.07 M ZnCl₂ and 0.02 M ZnCl₂ solutions were prepared for heavy metal removal test. This solution is basically a whitest type solution. Previously prepared graphene with SiO₂ (S2 composition) was heated at 300°C for 4 hours and ready to use for heavy metal removal.



Figure 4.16: 0.07 M whitish ZnCl₂ solution

4.6.2. Experimental Setup

Initially, preheated G-SiO₂ nanoparticles was mixed with the water containing salts of zinc and allowed to settle in water. An example, 2.5 gram of synthesized G-SiO₂ is treated with 50 ml 0.07M ZnCl₂ solution. The 0.07 M ZnCl₂ concentration displays a whitish color solution which turned to colorless within one or two hours of treatment with G-SiO₂ nanocomposites. As the time went by the solution became clearer. After six days the solution had been filtered.

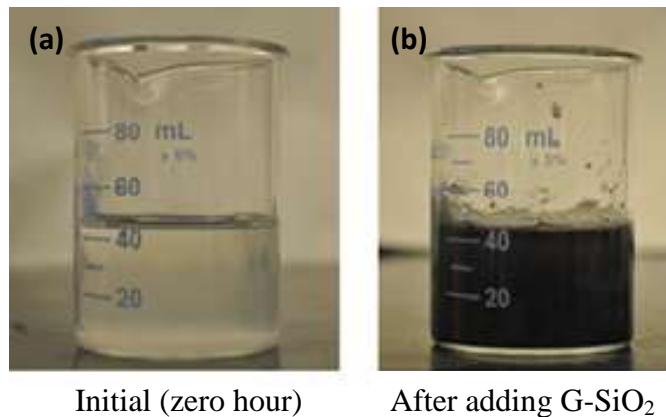


Figure 4.17: Initial 0.07 M ZnCl₂ solution (a) and same solution after adding G-SiO₂(b)

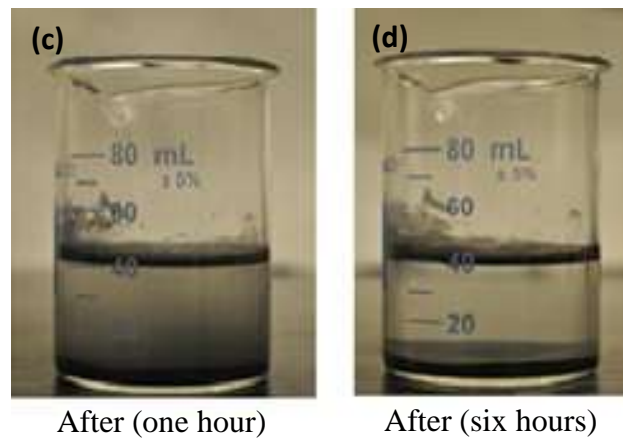
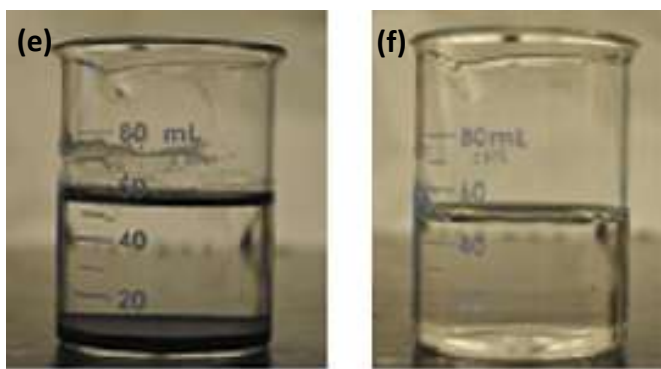


Figure 4.18: 0.07 M ZnCl₂ solution and G-SiO₂ after one hour(c) and six hours(d)



After (Six day)

After filtering

Figure 4.19: 0.07 M $ZnCl_2$ solution and G-SiO₂ after six days (e) and after filtering (f)

4.6.3 Finding of the Work

The presence of heavy metal was tested using electrochemical cyclic voltammetry (CV) technique. The CV measurement on the water treated with G-SiO₂ has been tested for several days to understand the presence of heavy metals in water.

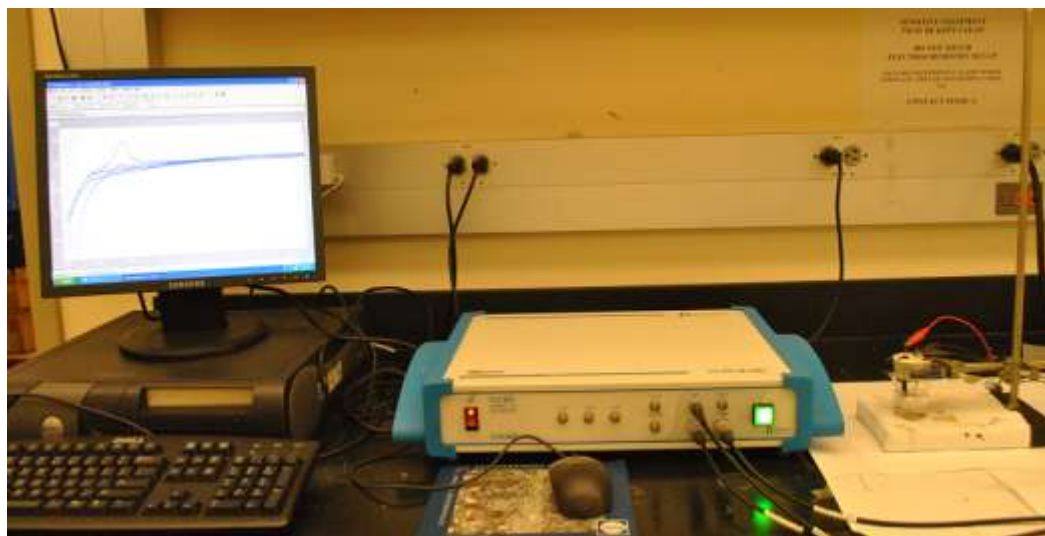


Figure 4.20: CV measurement to check the redox peak of Zn ion in the water.

Interestingly, the near complete separation had been observed by treating the heavy metal contaminated water sample for one to two days in presence of G-SiO₂ nanoparticles. The redox potential observed for the heavy metal had been found to diminish as a function of treatment with respect to time, and no redox peak was observed after the treatment for five to six days.

Further test using EDS measurement indicates that the heavy metal ions were observed within the G-SiO₂ nanocomposite. The recovery of G-SiO₂ nanocomposite was obtained by washing using deionized water. This experimental finding indicates that the G-SiO₂ nanocomposite could be exploited for potential heavy metals cleaning from waste or drinking water.

Table 4.2 Change of the redox peak value with respect to time for 0.07 M ZnCl₂

| Time (hour) | Peak($\mu\text{A}/\text{cm}^2$) | C/C ₀ |
|-------------|-----------------------------------|------------------|
| 1 | 160.68 | 1 |
| 2 | 155.3 | 0.96652 |
| 24 | 85.71 | 0.53342 |
| 72 | 62.83 | 0.39103 |
| 96 | 17.21 | 0.10711 |
| 120 | 15.15 | 0.09429 |
| 144 | 12.18 | 0.0758 |

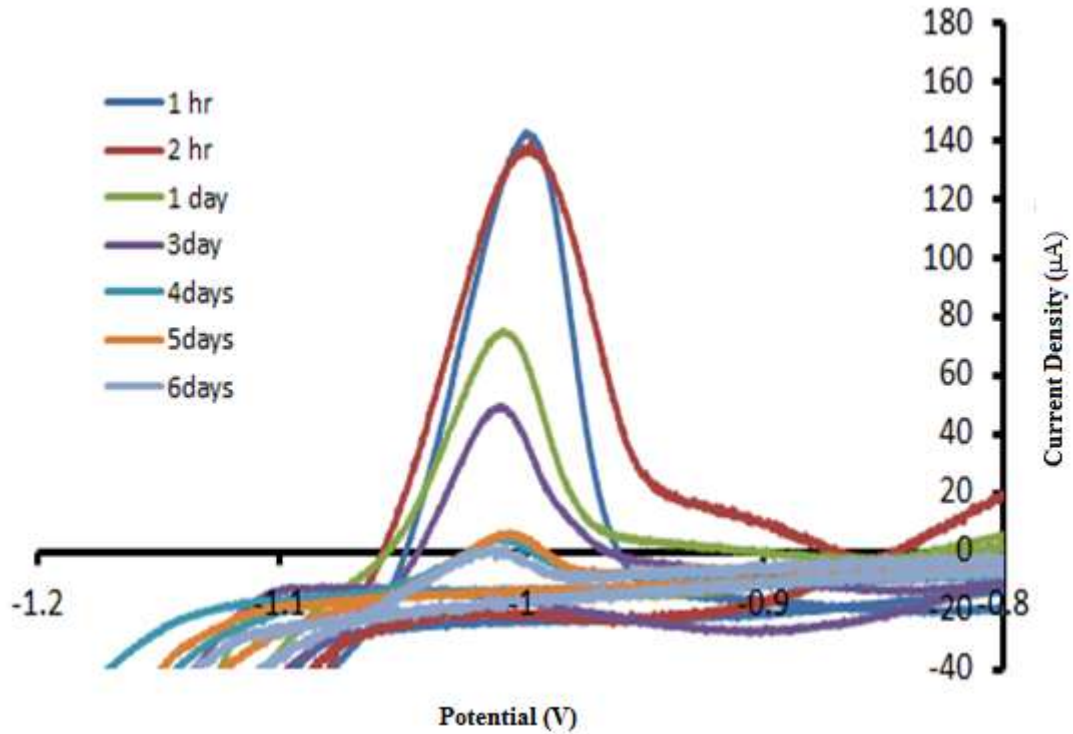


Figure 4.21: Reduction of the redox peak with respect to time.

It is considered that redox peak (A) is proportional to the concentration (C). So it can be assumed that change of the redox peak (A/A_0) indicates the change of the concentration (C/C_0) where, A_0 and C_0 were the initial redox peak and initial concentration respectively.

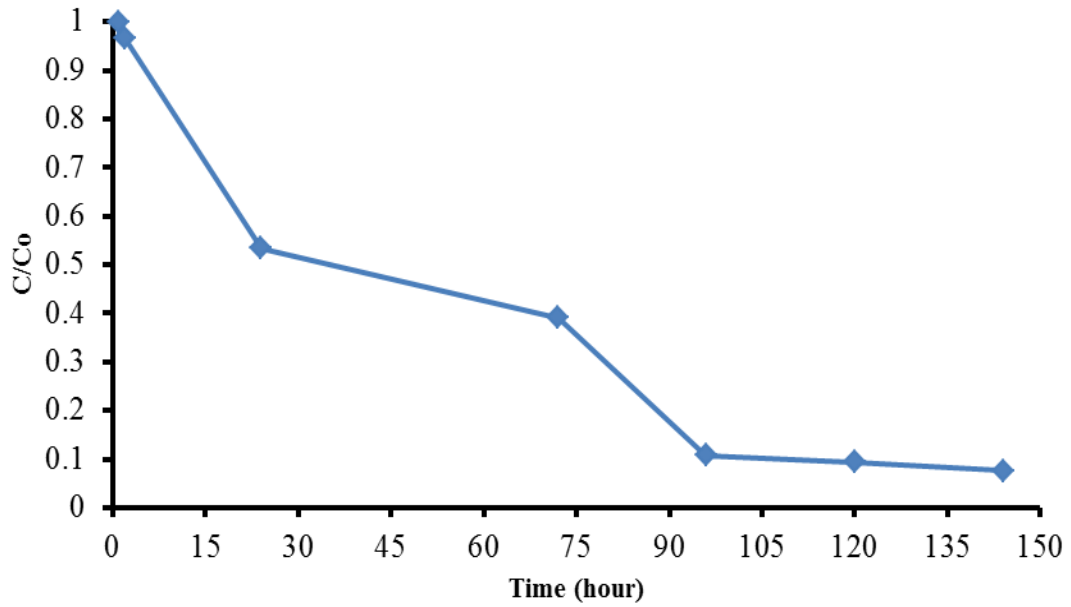


Figure 4.22: Adsorption of 0.07 M ZnCl₂ by G-SiO₂

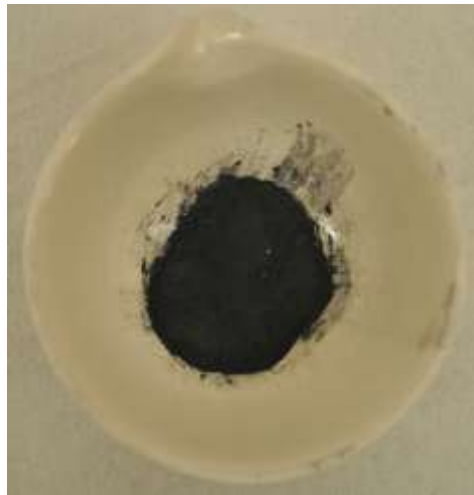


Figure 4.23: G-SiO₂ sample collected after filtering the solution

EDS measurement was done on the sample to check if the heavy metal ions was there. Figure 4.22 below indicates that the heavy metal ions were observed within the G-SiO₂ nanocomposite.

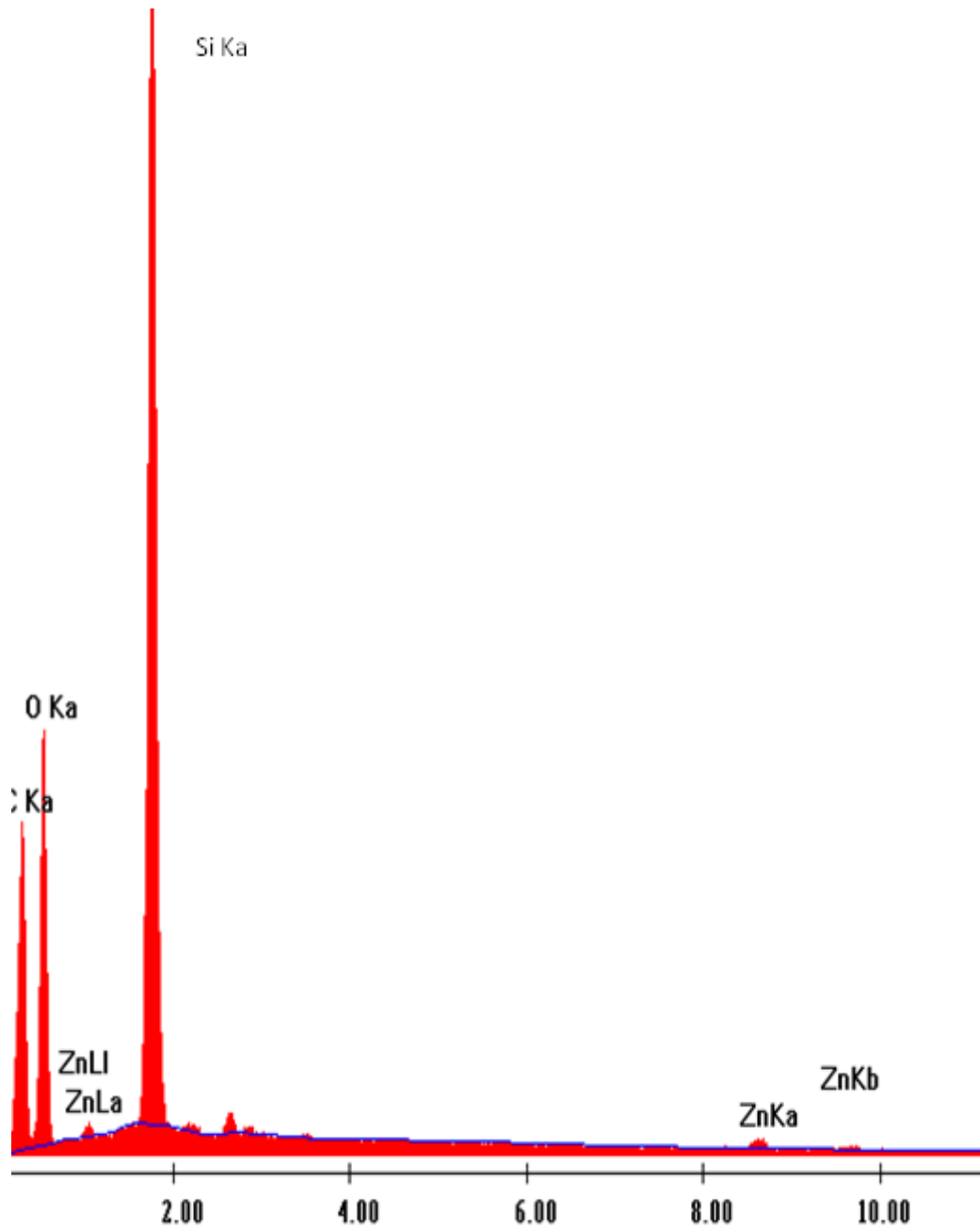


Figure 4.24: EDS of the filtered G-SiO₂ which shows Zn in the material.

The recovery of G-SiO₂ nanocomposite was obtained by washing using deionized water. This experimental finding indicates that the G-SiO₂ nanocomposite could be exploited for potential heavy metals cleaning from waste or drinking water.

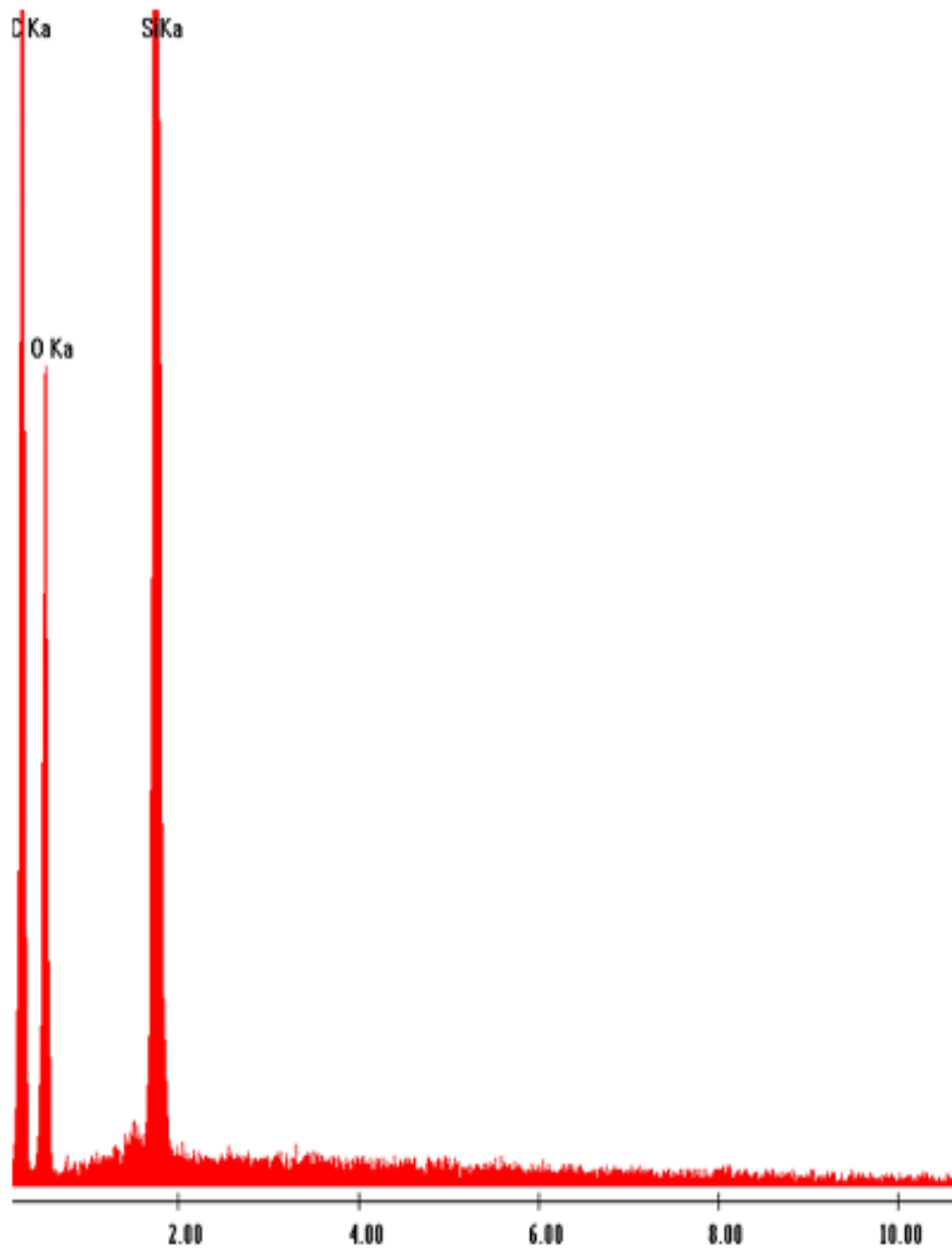


Figure 4.25: EDS of the filtered G-SiO₂ which is washed with deionized water

Same method was employed with ZnCl₂ solution of concentration of 0.02 M. We went through the same method and observed the same trend as 0.07 M ZnCl₂ solution.

The redox potential observed for the heavy metal had been found to diminish as a function of treatment with respect to time, and no redox peak was observed after the treatment for five to six days.

Table 4.3 Change of the redox peak value with respect to time for 0.02 M ZnCl₂

| Time (hour) | Peak($\mu\text{A}/\text{cm}^2$) | C/C ₀ |
|-------------|-----------------------------------|------------------|
| 0 | 51.83 | 1 |
| 5 | 19.1 | 0.3685 |
| 24 | 7.5 | 0.144 |
| 48 | 3.78 | 0.39103 |
| 72 | 2.1 | 0.073 |
| 96 | 1.98 | 0.038 |
| 120 | 1.75 | 0.033 |

It is considered that redox peak (A) is proportional to the concentration (C). So it can be assumed that change of the redox peak (A/A₀) indicates the change of the concentration (C/C₀) where, A₀ and C₀ were the initial redox peak and initial concentration respectively

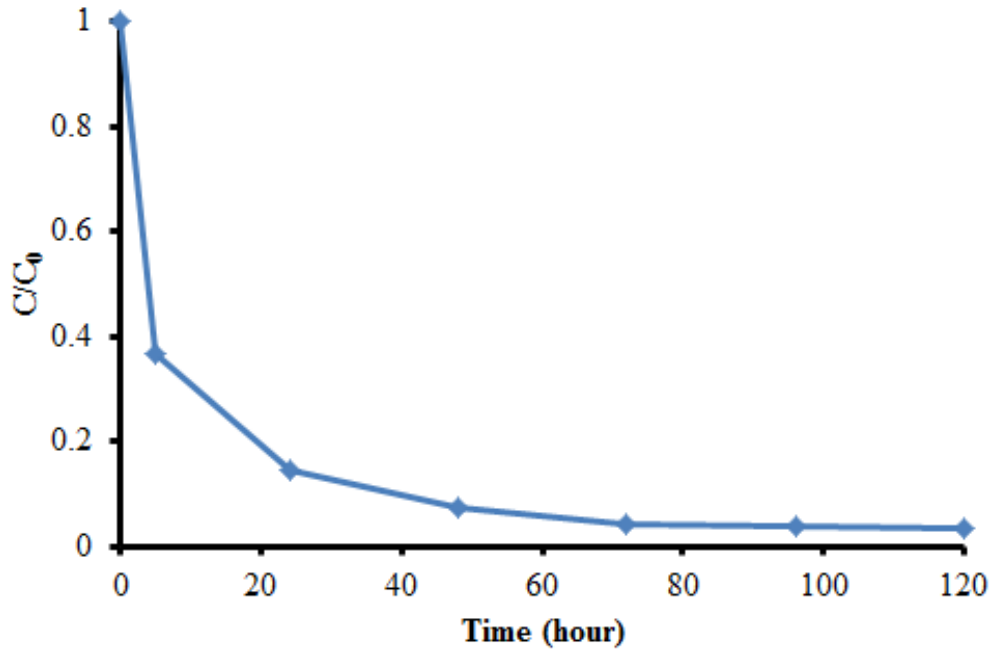


Figure 4.26: Adsorption of 0.02 M ZnCl₂ by G-SiO₂

4.7 Summary

It has been observed that Zn ions have been absorbed by the G-SiO₂ from the ZnCl₂ solution. EDS measurement shows that it has Zn particles in the filtered G-SiO₂ nanoparticles. We can reuse the G-SiO₂ just by washing the nanoparticles with ionized water.

4.8 References

- [1] A. K. Geim and K. S. Novoselov, "The rise of graphene," Nat Mater, vol. 6, no. 3, pp. 183-191, Mar. 2007.
- [2] J. C. Meyer, A. K. Geim, M. I. Katsnelson, K. S. Novoselov, T. J. Booth, and S. Roth, "The structure of suspended graphene sheets," Nature, vol. 446, no. 7131, pp. 60-63, Mar. 2007.

- [3] H.-P. HUANG and J.-J. ZHU, "Preparation of Novel Carbon-based Nanomaterial of Graphene and Its Applications Electrochemistry," Chinese Journal of Analytical Chemistry, vol. 39, no. 7, pp. 963-971, Jul. 2011.
- [4] A. H. C. Neto, F. Guinea, N. M. R. Peres, K. S. Novoselov, and A. K. Geim, "The electronic properties of graphene," arXiv:0709.1163, Sep. 2007.
- [5] D. A. C. Brownson, D. K. Kampouris, and C. E. Banks, "An overview of graphene in energy production and storage applications," Journal of Power Sources, vol. 196, no. 11, pp. 4873-4885, Jun. 2011.
- [6] Nan Meng, J. F. Fernandez, D. Vignaud, G. Dambrine, and H. Happy, "Fabrication and Characterization of an Epitaxial Graphene Nanoribbon-Based Field-Effect Transistor," IEEE Transactions on Electron Devices, vol. 58, no. 6, pp. 1594-1596, Jun. 2011.
- [7] Y. Shao, J. Wang, H. Wu, J. Liu, I. A. Aksay, and Y. Lin, "Graphene Based Electrochemical Sensors and Biosensors: A Review," Electroanalysis, vol. 22, no. 10, pp. 1027-1036, May 2010.
- [8] F. Schwierz, "Graphene transistors," Nat Nano, vol. 5, no. 7, pp. 487-496, Jul. 2010.
- [9] M. Ishigami, J. H. Chen, W. G. Cullen, M. S. Fuhrer, and E. D. Williams, "Atomic Structure of Graphene on SiO₂," Nano Letters, vol. 7, no. 6, pp. 1643-1648, Jun. 2007.
- [10] M. Z. Hossain, "Chemistry at the graphene-SiO₂ interface," Applied Physics Letters, vol. 95, p. 143125, 2009.
- [11] T. Kuilla, S. Bhadra, D. Yao, N. H. Kim, S. Bose, and J. H. Lee, "Recent advances in graphene based polymer composites," Progress in Polymer Science, vol. 35, no. 11, pp. 1350-1375, Nov. 2010.
- [12] J. Hofrichter et al., "Synthesis of Graphene on Silicon Dioxide by a Solid Carbon Source," Nano Letters, vol. 10, no. 1, pp. 36-42, Jan. 2010.
- [13] I Calizo, D Teweldebrhan W Bao, F Miao, C N Lau and A A Balandin Spectroscopic Raman Nanometrology of Graphene and Graphene Multilayers on Arbitrary Substrates Journal of Physics: Conference Series 109 (2008) 012008

- [14] C. Stampfer, a F. Molitor, D. Graf, and K. Ensslin Raman imaging of doping domains in graphene on SiO₂, Applied Physics Letters 91, 241907 2007

Chapter 5

Conclusion and Future Recommendation

Existence of life depends upon the availability of the water. From early civilizations, it has been found that economic development rotate with the accessibility of quality water production. Civilization has moved from one place to another place in search of pure water.

Water is getting polluted by the presence of natural organic materials, heavy metals (Cd, Zn, Cu, Pb, Zn, As Al, Be, and Ag) as well as industrial pollutants (pesticides, heavy metals, micro-organisms). Water should be free from metals (Cd, Zn, Cu, Pb, Zn, As Al, Be, and Ag) and organics (e.g., antibiotics, chloroacetic, Chlorine, ozone, chlorine dioxide, and chloramine). Unavailability of pure drinking water is a critical problem all over the world. According to WHO, millions of people die from diarrheal diseases every year, and billions of people has lack of access to safe drinking water. Hence, it becomes clear and specific that scientific discovery for making novel materials and their commercialization is the call of present situation. It is an important goal for state-of-the-art science to concentrate their attention on developing preventative technologies for improving the grievous effect on the environment. This goal can only be achieved by discovering novel materials with unusual properties.

5.1 Organic Material Remediation

In conclusion, we have successfully synthesized the G-TiO₂ using sol-gel method. From TEM, it has been observed that graphene sheets are heavily covered with TiO₂ particles and distributed on the graphene sheets with an obvious shift of the absorption edge in the UV-vis absorption spectrum. XRD patterns show that the crystal structure of the sample is anatase. Raman spectroscopy also indicates that it has G-TiO₂ in the form of anatase. Like typical of graphene D- peak, G-peak and 2D-peak has been seen in the sample. The feasibility of removing organic materials from water by using G-TiO₂ composites as photocatalyst is demonstrated in this paper. The resulting hybrid material shows superior photocatalytic activity. The photodegradation of MO is carried out by using different photocatalysts like G-TiO₂, P25 (commercially available TiO₂) under irradiation of simulated sunlight and compared. We have also tested and compared the G-SiO₂ for photodegradation of MO. The G-TiO₂ composite shows excellent photocatalytic activity. The G-SiO₂ nanocomposite doesn't show significant photodegradation like G-TiO₂. The results presented in this paper demonstrated that G-TiO₂ is a very promising candidate for development of high performance photocatalysts. Such intriguing composites may find significant applications in environmental protection.

5.2 Heavy Metal Removal

The nanocomposite materials of G-SiO₂ were synthesized by using different ratio of G to TEOS using sole-gel process. The increase of graphene in SiO₂ shows more grains type of structure whereas the larger graphene variation shows the flakes and woolen type of structure in G-SiO₂ nanocomposite. The interesting features of bundling

study shows diffusional controlled CV system for the increase of graphene in G-SiO₂ samples. The G-SiO₂ nanocomposite has been found to be highly conducting with only less than 2% of graphene in the nanocomposite. The semiconductor to metallic transition is observed by varying the graphene content with SiO₂ precursor for synthesis of G-SiO₂ nanocomposite. The physical and electrical characteristics of G-SiO₂ are indicative that it is the future material electrical applications. In this experiment, G-SiO₂ is employed to absorb the heavy metal from Zn ion from solution of different concentrations. The presence of heavy metal is tested using electrochemical cyclic voltammetry (CV) technique. The water treated with G-SiO₂ has been tested using CV measurement for several days to understand the presence of heavy metals in water. The redox potential observed for the heavy metal has been found to diminish as a function of treatment with respect to time, and very tiny redox peak is observed after the treatment for four to five days. Further test using EDS measurement indicates that the heavy metal ions are observed within the G-SiO₂ nanocomposite. The recovery of G-SiO₂ nanocomposite is obtained by washing using deionized water. Our experimental finding indicates that the G-SiO₂ nanocomposite could be exploited for potential heavy metals cleaning from waste or drinking water and could be quite effective to develop a technique to remove heavy metal from water. The G-SiO₂ nanocomposite doesn't show significant photodegradation like G-TiO₂ but that is promising as G-SiO₂ can also remove heavy metal from water.

5.3 Future Recommendation

For the Organic material remediation by using G-TiO₂, we experimented with single ratio of Graphene and TiO₂. In future, we can work with different ratio and can see what type of variation it shows in photodegradation process. We used only Methyl Orange as our organic material, which we removed from water with an adequate time. In future, we can also work with Dichlorobenzene, methyl blue and many more organic materials to see the time required to decontaminate the water by using different ratio of G-TiO₂. Also, we can vary the intensity to see the fluctuation of time needed for the remediation process of water.

For the heavy metal removal process by using G-SiO₂, we only removed the Zn ion from the water. In future, we can try other heavy metals like Cd, Pd, Sn Cr and As ions to remove from the water to justify the effectiveness of this technique. We can also introduce the mass spectroscopy to measure the presence of heavy metal.

The aim of these experiments are to give an overall perspective of the use of Graphene Metal Oxide nanoparticles, to treat the contaminated water for drinking and reuse more effectively, than through conventional ways.

Appendix A: Permissions

4/12/12

Rightlink Printable License

NATURE PUBLISHING GROUP LICENSE TERMS AND CONDITIONS

Apr 12, 2012

This is a License Agreement between Tanvir E Alam ("You") and Nature Publishing Group ("Nature Publishing Group") provided by Copyright Clearance Center ("CCC"). The license consists of your order details, the terms and conditions provided by Nature Publishing Group, and the payment terms and conditions.

All payments must be made in full to CCC. For payment instructions, please see information listed at the bottom of this form.

| | |
|--|--|
| License Number | 2886640007612 |
| License date | Apr 12, 2012 |
| Licensed content publisher | Nature Publishing Group |
| Licensed content publication | Nature Materials |
| Licensed content title | The rise of graphene |
| Licensed content author | A. K. Geim and K. S. Novoselov |
| Licensed content date | Mar 1, 2007 |
| Volume number | 6 |
| Issue number | 3 |
| Type of Use | reuse in a thesis/dissertation |
| Requestor type | academic/educational |
| Format | print and electronic |
| Portion | figures/tables/illustrations |
| Number of figures/tables/illustrations | 1 |
| High-res required | no |
| Figures | Figure 1 Mother of all graphitic forms. Graphene is a 2D building material for carbon materials of all other dimensionalities. It can be wrapped up into 0D buckyballs, rolled into 1D nanotubes or stacked into 3D graphite |
| Author of this NPG article | no |
| Your reference number | |
| Title of your thesis / dissertation | Metal Oxide Graphene Nanocomposites for Organic and Heavy Metal Remediation Application |
| Expected completion date | May 2012 |
| Estimated size (number of pages) | 97 |
| Total | 0.00 USD |
| Terms and Conditions | |

<https://s100.copyright.com/AppDispatchServlet>

1/4

Appendix A (Continued)

4/12/12

Rightlink Printable License

Terms and Conditions for Permissions

Nature Publishing Group hereby grants you a non-exclusive license to reproduce this material for this purpose, and for no other use, subject to the conditions below:

1. NPG warrants that it has, to the best of its knowledge, the rights to license reuse of this material. However, you should ensure that the material you are requesting is original to Nature Publishing Group and does not carry the copyright of another entity (as credited in the published version). If the credit line on any part of the material you have requested indicates that it was reprinted or adapted by NPG with permission from another source, then you should also seek permission from that source to reuse the material.
2. Permission granted free of charge for material in print is also usually granted for any electronic version of that work, provided that the material is incidental to the work as a whole and that the electronic version is essentially equivalent to, or substitutes for, the print version. Where print permission has been granted for a fee, separate permission must be obtained for any additional, electronic re-use (unless, as in the case of a full paper, this has already been accounted for during your initial request in the calculation of a print run). NB: In all cases, web-based use of full-text articles must be authorized separately through the 'Use on a Web Site' option when requesting permission.
3. Permission granted for a first edition does not apply to second and subsequent editions and for editions in other languages (except for signatories to the STM Permissions Guidelines, or where the first edition permission was granted for free).
4. Nature Publishing Group's permission must be acknowledged next to the figure, table or abstract in print. In electronic form, this acknowledgement must be visible at the same time as the figure/table/abstract, and must be hyperlinked to the journal's homepage.
5. The credit line should read:
Reprinted by permission from Macmillan Publishers Ltd: [JOURNAL NAME] (reference citation), copyright (year of publication)
For AOP papers, the credit line should read:
Reprinted by permission from Macmillan Publishers Ltd: [JOURNAL NAME], advance online publication, day month year (doi: 10.1038/sj.[JOURNAL ACRONYM].XXXXX)

Note: For republication from the *British Journal of Cancer*, the following credit lines apply.

Reprinted by permission from Macmillan Publishers Ltd on behalf of Cancer Research UK: [JOURNAL NAME] (reference citation), copyright (year of publication) For AOP papers, the credit line should read:

Reprinted by permission from Macmillan Publishers Ltd on behalf of Cancer Research UK: [JOURNAL NAME], advance online publication, day month year (doi: 10.1038/sj.[JOURNAL ACRONYM].XXXXX)

<https://s100.copyright.com/AppDispatchServlet>

2/4

Appendix A (Continued)

4/12/12

Rightslink Printable License

6. Adaptations of single figures do not require NPG approval. However, the adaptation should be credited as follows:

Adapted by permission from Macmillan Publishers Ltd: [JOURNAL NAME] (reference citation), copyright (year of publication)

Note: For adaptation from the *British Journal of Cancer*, the following credit line applies.

Adapted by permission from Macmillan Publishers Ltd on behalf of Cancer Research UK: [JOURNAL NAME] (reference citation), copyright (year of publication)

7. Translations of 401 words up to a whole article require NPG approval. Please visit <http://www.macmillanmedicalcommunications.com> for more information. Translations of up to a 400 words do not require NPG approval. The translation should be credited as follows:

Translated by permission from Macmillan Publishers Ltd: [JOURNAL NAME] (reference citation), copyright (year of publication).

Note: For translation from the *British Journal of Cancer*, the following credit line applies.

Translated by permission from Macmillan Publishers Ltd on behalf of Cancer Research UK: [JOURNAL NAME] (reference citation), copyright (year of publication)

We are certain that all parties will benefit from this agreement and wish you the best in the use of this material. Thank you.

Special Terms:

v1.1

If you would like to pay for this license now, please remit this license along with your payment made payable to "COPYRIGHT CLEARANCE CENTER" otherwise you will be invoiced within 48 hours of the license date. Payment should be in the form of a check or money order referencing your account number and this invoice number RLNK500759390. Once you receive your invoice for this order, you may pay your invoice by credit card. Please follow instructions provided at that time.

**Make Payment To:
Copyright Clearance Center
Dept 001
P.O. Box 843006
Boston, MA 02284-3006**

For suggestions or comments regarding this order, contact RightsLink Customer Support: customercare@copyright.com or +1-877-622-5543 (toll free in the US) or +1-978-646-2777.

Gratis licenses (referencing \$0 in the Total field) are free. Please retain this printable license for your reference. No payment is required.

<https://e100.copyright.com/AppDispatchServlet>

3/4

Appendix A (Continued)

4/12/12

Rightlink Printable License

ELSEVIER LICENSE TERMS AND CONDITIONS

Apr 12, 2012

This is a License Agreement between Tanvir E Alam ("You") and Elsevier ("Elsevier") provided by Copyright Clearance Center ("CCC"). The license consists of your order details, the terms and conditions provided by Elsevier, and the payment terms and conditions.

All payments must be made in full to CCC. For payment instructions, please see information listed at the bottom of this form.

| | |
|--|--|
| Supplier | Elsevier Limited The Boulevard, Langford Lane Kidlington, Oxford, OX5 1GB, UK |
| Registered Company Number | 1982084 |
| Customer name | Tanvir E Alam |
| Customer address | 15501 Bruce B Downs Blvd, apt-3906 Tampa, FL 33647 |
| License number | 2886641199401 |
| License date | Apr 12, 2012 |
| Licensed content publisher | Elsevier |
| Licensed content publication | Desalination |
| Licensed content title | Heterogeneous photocatalytic degradation of phenols in wastewater: A review on current status and developments |
| Licensed content author | Saber Ahmed, M.G. Rasul, Wayde N. Martens, R. Brown, M.A. Hashib |
| Licensed content date | 15 October 2010 |
| Licensed content volume number | 261 |
| Licensed content issue number | 1-2 |
| Number of pages | 16 |
| Start Page | 3 |
| End Page | 18 |
| Type of Use | reuse in a thesis/dissertation |
| Intended publisher of new work | other |
| Portion | figures/tables/illustrations |
| Number of figures/tables/illustrations | 1 |
| Format | both print and electronic |
| Are you the author of this Elsevier article? | No |

<https://s100.copyright.com/AppDispatchServlet>

1/5

Appendix A (Continued)

| | |
|-----------------------------------|---|
| 4/12/12 | Rightlink Printable License |
| Will you be translating? | No |
| Order reference number | |
| Title of your thesis/dissertation | Metal Oxide Graphene Nanocomposites for Organic and Heavy Metal Remediation Application |
| Expected completion date | May 2012 |
| Estimated size (number of pages) | 97 |
| Elsevier VAT number | GB 494 6272 12 |
| Permissions price | 0.00 USD |
| VAT/Local Sales Tax | 0.0 USD / 0.0 GBP |
| Total | 0.00 USD |
| Terms and Conditions | |

INTRODUCTION

1. The publisher for this copyrighted material is Elsevier. By clicking "accept" in connection with completing this licensing transaction, you agree that the following terms and conditions apply to this transaction (along with the Billing and Payment terms and conditions established by Copyright Clearance Center, Inc. ("CCC"), at the time that you opened your Rightslink account and that are available at any time at <http://myaccount.copyright.com>).

GENERAL TERMS

2. Elsevier hereby grants you permission to reproduce the aforementioned material subject to the terms and conditions indicated.
3. Acknowledgement: If any part of the material to be used (for example, figures) has appeared in our publication with credit or acknowledgement to another source, permission must also be sought from that source. If such permission is not obtained then that material may not be included in your publication/copies. Suitable acknowledgement to the source must be made, either as a footnote or in a reference list at the end of your publication, as follows:

"Reprinted from Publication title, Vol /edition number, Author(s), Title of article / title of chapter, Pages No., Copyright (Year), with permission from Elsevier [OR APPLICABLE SOCIETY COPYRIGHT OWNER]." Also Lancet special credit - "Reprinted from The Lancet, Vol. number, Author(s), Title of article, Pages No., Copyright (Year), with permission from Elsevier."
4. Reproduction of this material is confined to the purpose and/or media for which permission is hereby given.
5. Altering/Modifying Material: Not Permitted. However figures and illustrations may be altered/adapted minimally to serve your work. Any other abbreviations, additions, deletions and/or any other alterations shall be made only with prior written authorization of Elsevier Ltd. (Please contact Elsevier at permissions@elsevier.com)
6. If the permission fee for the requested use of our material is waived in this instance, please be advised that your future requests for Elsevier materials may attract a fee.

Appendix A (Continued)

4/12/12

Rightlink Printable License

7. **Reservation of Rights:** Publisher reserves all rights not specifically granted in the combination of (i) the license details provided by you and accepted in the course of this licensing transaction, (ii) these terms and conditions and (iii) CCC's Billing and Payment terms and conditions.

8. **License Contingent Upon Payment:** While you may exercise the rights licensed immediately upon issuance of the license at the end of the licensing process for the transaction, provided that you have disclosed complete and accurate details of your proposed use, no license is finally effective unless and until full payment is received from you (either by publisher or by CCC) as provided in CCC's Billing and Payment terms and conditions. If full payment is not received on a timely basis, then any license preliminarily granted shall be deemed automatically revoked and shall be void as if never granted. Further, in the event that you breach any of these terms and conditions or any of CCC's Billing and Payment terms and conditions, the license is automatically revoked and shall be void as if never granted. Use of materials as described in a revoked license, as well as any use of the materials beyond the scope of an unrevoked license, may constitute copyright infringement and publisher reserves the right to take any and all action to protect its copyright in the materials.

9. **Warranties:** Publisher makes no representations or warranties with respect to the licensed material.

10. **Indemnity:** You hereby indemnify and agree to hold harmless publisher and CCC, and their respective officers, directors, employees and agents, from and against any and all claims arising out of your use of the licensed material other than as specifically authorized pursuant to this license.

11. **No Transfer of License:** This license is personal to you and may not be sublicensed, assigned, or transferred by you to any other person without publisher's written permission.

12. **No Amendment Except in Writing:** This license may not be amended except in a writing signed by both parties (or, in the case of publisher, by CCC on publisher's behalf).

13. **Objection to Contrary Terms:** Publisher hereby objects to any terms contained in any purchase order, acknowledgment, check endorsement or other writing prepared by you, which terms are inconsistent with these terms and conditions or CCC's Billing and Payment terms and conditions. These terms and conditions, together with CCC's Billing and Payment terms and conditions (which are incorporated herein), comprise the entire agreement between you and publisher (and CCC) concerning this licensing transaction. In the event of any conflict between your obligations established by these terms and conditions and those established by CCC's Billing and Payment terms and conditions, these terms and conditions shall control.

14. **Revocation:** Elsevier or Copyright Clearance Center may deny the permissions described in this License at their sole discretion, for any reason or no reason, with a full refund payable to you. Notice of such denial will be made using the contact information provided by you. Failure to receive such notice will not alter or invalidate the denial. In no event will Elsevier or Copyright Clearance Center be responsible or liable for any costs, expenses or damage incurred by you as a result of a denial of your permission request, other than a refund of the amount(s) paid by you to Elsevier and/or Copyright Clearance Center for denied permissions.

LIMITED LICENSE

<https://s100.copyright.com/AppDispatchServlet>

3/5

Appendix A (Continued)

4/12/12

Rightlink Printable License

The following terms and conditions apply only to specific license types:

15. Translation: This permission is granted for non-exclusive world **English** rights only unless your license was granted for translation rights. If you licensed translation rights you may only translate this content into the languages you requested. A professional translator must perform all translations and reproduce the content word for word preserving the integrity of the article. If this license is to re-use 1 or 2 figures then permission is granted for non-exclusive world rights in all languages.

16. Website: The following terms and conditions apply to electronic reserve and author websites:
Electronic reserve: If licensed material is to be posted to website, the web site is to be password-protected and made available only to bona fide students registered on a relevant course if

This license was made in connection with a course,

This permission is granted for 1 year only. You may obtain a license for future website posting. All content posted to the web site must maintain the copyright information line on the bottom of each image,

A hyper-text must be included to the Homepage of the journal from which you are licensing at <http://www.sciencedirect.com/science/journal/xxxxx> or the Elsevier homepage for books at <http://www.elsevier.com> , and

Central Storage: This license does not include permission for a scanned version of the material to be stored in a central repository such as that provided by Heron/XanEdu.

17. Author website for journals with the following additional clauses:

All content posted to the web site must maintain the copyright information line on the bottom of each image, and

the permission granted is limited to the personal version of your paper. You are not allowed to download and post the published electronic version of your article (whether PDF or HTML, proof or final version), nor may you scan the printed edition to create an electronic version,

A hyper-text must be included to the Homepage of the journal from which you are licensing at <http://www.sciencedirect.com/science/journal/xxxxx> , As part of our normal production process, you will receive an e-mail notice when your article appears on Elsevier's online service ScienceDirect (www.sciencedirect.com). That e-mail will include the article's Digital Object Identifier (DOI). This number provides the electronic link to the published article and should be included in the posting of your personal version. We ask that you wait until you receive this e-mail and have the DOI to do any posting.

Central Storage: This license does not include permission for a scanned version of the material to be stored in a central repository such as that provided by Heron/XanEdu.

18. Author website for books with the following additional clauses:

Authors are permitted to place a brief summary of their work online only.

A hyper-text must be included to the Elsevier homepage at <http://www.elsevier.com>

All content posted to the web site must maintain the copyright information line on the bottom of each image

You are not allowed to download and post the published electronic version of your chapter, nor

<https://s100.copyright.com/AppDispatchServlet>

4/5

Appendix A (Continued)

4/12/12

Rightlink Printable License

may you scan the printed edition to create an electronic version.

Central Storage: This license does not include permission for a scanned version of the material to be stored in a central repository such as that provided by Heron/XanEdu.

19. **Website** (regular and for author): A hyper-text must be included to the Homepage of the journal from which you are licensing at <http://www.sciencedirect.com/science/journal/xxxxx> or for books to the Elsevier homepage at <http://www.elsevier.com>

20. **Thesis/Dissertation**: If your license is for use in a thesis/dissertation your thesis may be submitted to your institution in either print or electronic form. Should your thesis be published commercially, please reapply for permission. These requirements include permission for the Library and Archives of Canada to supply single copies, on demand, of the complete thesis and include permission for UMI to supply single copies, on demand, of the complete thesis. Should your thesis be published commercially, please reapply for permission.

21. **Other Conditions**:

v1.6

If you would like to pay for this license now, please remit this license along with your payment made payable to "COPYRIGHT CLEARANCE CENTER" otherwise you will be invoiced within 48 hours of the license date. Payment should be in the form of a check or money order referencing your account number and this invoice number RLNK500759399. Once you receive your invoice for this order, you may pay your invoice by credit card. Please follow instructions provided at that time.

**Make Payment To:
Copyright Clearance Center
Dept 001
P.O. Box 843006
Boston, MA 02284-3006**

For suggestions or comments regarding this order, contact RightsLink Customer Support: customercare@copyright.com or +1-877-622-5543 (toll free in the US) or +1-978-646-2777.

Gratis licenses (referencing \$0 in the Total field) are free. Please retain this printable license for your reference. No payment is required.